SOME PROPERTIES OF VIBRATING TELEPHONE DIAPHRAGMS.

By A. E. KENNELLY, S.D., A.M., and H. O. TAYLOR, Ph.D.

(*Read April 14, 1916.*)

This investigation was conducted by the Research Division of the Electrical Engineering Department, of the Massachusetts Institute of Technology, during the years 1915–16, under an appropriation from the American Telephone and Telegraph Company. The experimental work was carried on at Pierce Hall, Harvard University. It constitutes a continuation of the researches reported by the same authors in the paper read last year before the American Philosophical Society,[1] and in the paper by Kennelly and Affel, read last year before the American Academy of Arts and Sciences,[2] dealing with the motional-impedance circle of telephone receivers.

It is now well established that the motional-impedance circle of a telephone receiver; *i. e.*, the circular locus of that part of a receiver's impedance which is due to the motion of the diaphragm, enables the characteristic constants A, m, r and s of the instrument to be determined experimentally. Its diameter, OD, Fig. 4, is depressed below the resistance axis OA (resistance component of impedance), through a certain angle, AOD, which is designated by $\beta_1^\circ + \beta_2^\circ$. Here β_1° is regarded as the angle of lag of the pull on the diaphragm behind the alternating current in the coils giving rise thereto; while β_2° is regarded as the angle of lag of the E.M.F. induced in the coils, behind the velocity of the diaphragm's vibrational motion producing it.

The researches here reported have been two-fold namely:

1 "Explorations over the Vibrating Surfaces of Telephonic Diaphragms under Simple, Impressed Tones," by A. E. Kennelly and H. O. Taylor, *Proc. Am. Philos. Soc.*, Vol. LIV., April 22, 1915.

2 Bibliography, 10.

1. Investigations were made with a view to ascertaining how the two lag angles, β_1^0 and β_2^0 compared with each other, in a given receiver, and to what extent they depended upon the impressed frequency and upon variations in construction.

2. In the course of this research, which has involved the observation and plotting of some sixty motional-impedance circles, certain departures from the circle were noted, due to abnormalities or irregularities in the mechanics of the receiver diaphragm under test. Investigation was directed towards determining the nature and causes of these departures.

1. Investigation of the Depression Angles β_1^0 and β_2^0.

The method adopted for investigating the magnitudes of the two component depression angles β_1^0 and β_2^0 was an optical one, involving Lissajous figures.[3] A small and powerful beam of light

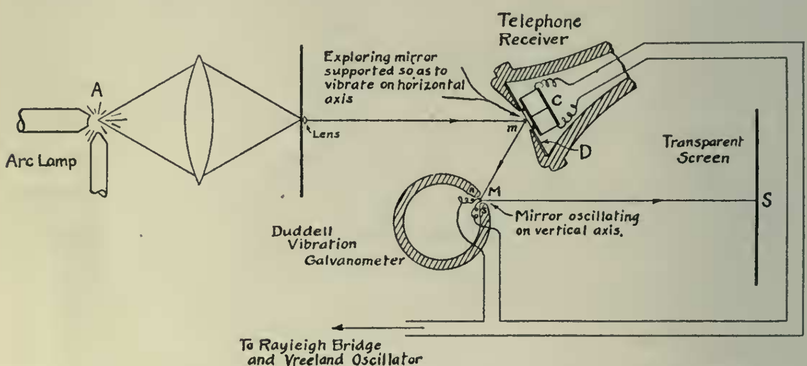

Fig. 1. Diagram of Optical System for Producing Lissajous' Figures.

from an arc lamp, *A*, Fig. 1, was directed onto a tiny triangular exploring mirror, about 0.5 mm. in length of edge *m*, as referred to in both of the preceding papers of this research.[4] This mirror was elastically supported in contact with the center of the outer surface of the telephone diaphragm *D*, so that vibratory displacements of the latter would cause the mirror, *m*, to rock about a horizontal

[3] Bibliography, 1.

[4] Bibliography, 9 and 10.

axis. The reflected arc-light beam then fell upon the mirror M, of a Duddell bifilar vibration galvanometer,[5] in the same circuit as the telephone receiver coils C, and so arranged as to vibrate about a vertical axis, under the action of the current which actuated the telephone. The beam finally produced a spot of light on the transparent screen, S. Owing to the two independent mirror vibrations being of the same frequency, but about mutually perpendicular axes, this spot of light traced Lissajous figures on the screen, and the observed shape of these figures enabled calculations to be made as to the phase differences between the movements of the two mirrors m and M. It was therefore necessary to make an initial examination into the phase relations of the Duddell galvanometer mirror M, with respect to the alternating current operating it.

Observations on the phase relations of vibration galvanometer mirrors have already been published.[6] It was found, however, in the research here reported, that as might be expected from the differential equation of motion of such an instrument as an oscillograph or vibration galvanometer, it inherently possesses a motional-impedance circle, like a telephone receiver. The motional-impedance circle of a vibration galvanometer, or an oscillograph, differs from that of the ordinary telephone receiver, in having its diameter coincident with the resistance axis, or very nearly so; so that $\beta_1^0 = \beta_2^0 = 0$. This means that the vibrational angular velocity at resonance is in phase with the vibromotive force, which in this case is also in phase with the actuating alternating current. From an observation of the instrument's motional-impedance circle and deflections, the essential mechanical and electrical constants of the instrument, for its particular state of adjustment, can be readily determined. This theory and technique for vibration instruments, which are only side issues of the main research here reported, are discussed in Appendix I. It suffices here to note that provided the Duddell galvanometer is out of tune, even only a few per cent. with respect to the actuating currents, its mirror displacements will be substantially either in phase with, or in opposite phase to, the ac-

[5] Bibliography, 5.
[6] Bibliography, 6.

tuating current. If the alternating current has a lower frequency than the particular resonant frequency to which the instrument is adjusted, the mirror displacements will be substantially in phase with the current; whereas if the A.C. frequency is higher than the

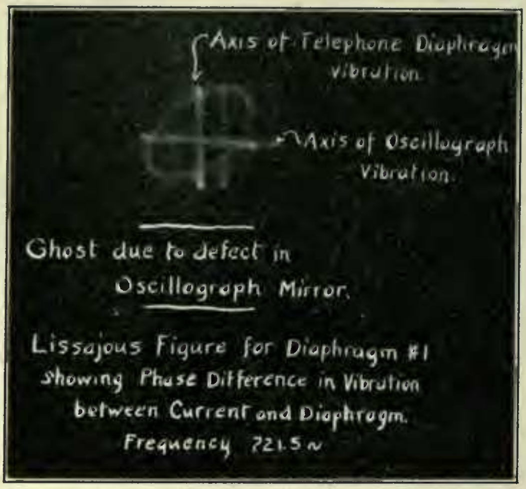

Fig. 2.

instrument's resonant frequency, the mirror displacements will be in opposite phase to the current. There was therefore no practical difficulty in ensuring one or the other of these two conditions, as might be desired, for impressed alternating-current frequencies up to 1,500 $\sim$, the Duddell galvanometer employed having a range from 100 to 2,000 $\sim$.

Fig. 2 is a photographic record of a Lissajous figure, obtained on the screen S of Fig. 1, for a particular case. These test records were photographed and analyzed. The well-known analysis is reproduced in Fig. 3. The Lissajous ellipse $ABCD$ about the center o and coördinate axes Xx and Yy, is supposed to be described in the direction of the arrows. Corresponding points on the circles $A_1B_1C_1D_1$ and $A_2B_2C_2D_2$, are projections from the ellipse on the Y and X axes respectively. The phase difference between the simple harmonic motions of Yy and Xx is any one of the four equal angles α_1, α_2, α_3, and α_4. Owing to imperfections in the photographic record and tracing process, these four angles ordinarily are not quite equal; but their arithmetical mean may be taken as the observed phase difference. Since in the photographic record, the oscillations

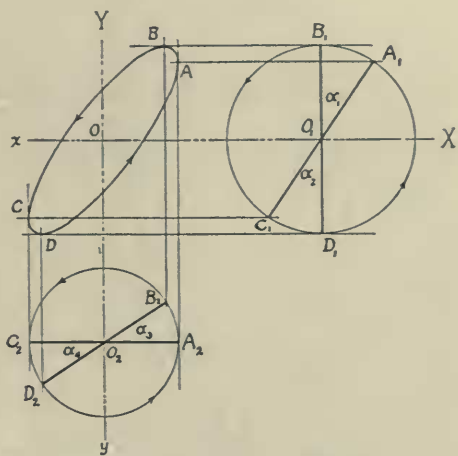

FIG. 3. Lissajous' Diagram.

of the telephone diaphragm produce the vertical component, and the oscillations of the galvanometer mirror (in phase with the current), produce the horizontal component, the lag of the diaphragm vibration behind the current becomes determined. This lag angle should agree with the lag computed by mechanical impedance ($90^\circ - \alpha^\circ$), except for the angle $\beta_1{}^\circ$. It was found that by varying the impressed A. C. frequency, the Lissajous ellipse could be made to pass through all its forms, *i. e.,* straight line, ellipse, circle, ellipse and straight line. The particular form offering easiest recognition and greatest precision of measurement, is the straight line, under which condition the two displacements are in either cophase or opposition. This means that the diaphragm displacement would be in $\pm$ cophase with the current, or the diaphragm velocity in quadrature with the current. Referring to Fig. 4, OA represents the standard phase of A. C. vector current. OB, in quadrature therewith, is the phase of the diaphragm's vibrational velocity when the Lissajous figure is a straight line. By observing, on the Rayleigh bridge, the motional impedance OC of the telephone at this frequency, the angle BOC is the lag of the motional E. M. F. behind the velocity producing it, and is equal to the angle β_2^0. Since the

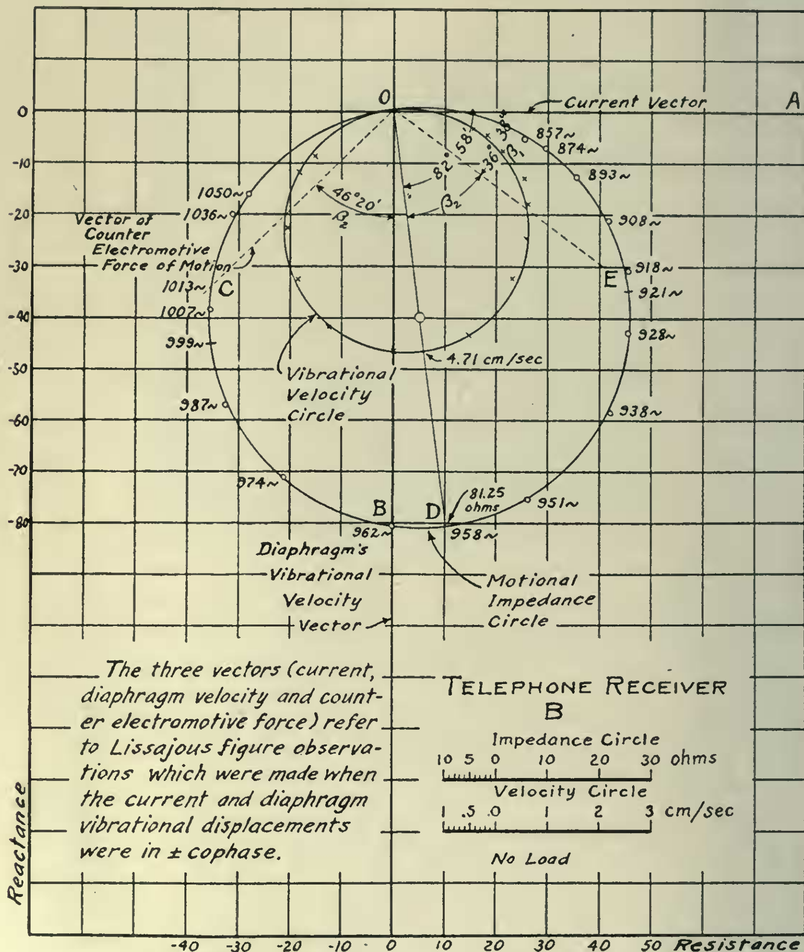

FIG. 4. Undistorted Circles of Motional-Impedance and Velocity.

depression angle AOD of the motional impedance circle, taken from the observation plot is $\beta_1^0 + \beta_2^0$, the angle β_1^0 is immediately determined. The test therefore requires the motional-impedance circle to be obtained over the principal range of frequencies, in Fig. 4 from

857 ~ to 1,050 ~, then adjusting the frequency to the particular value (1,013 ~) at which the Lissajous figure becomes a straight line, measuring the motional impedance in the circle at this point, and then deducing $\beta_2{}^0$ and $\beta_1{}^0$ geometrically. In the case of Fig. 4, $\beta_1{}^0 = 36° \ 38'$ and $\beta_2{}^0 = 46° \ 20'$. The precision obtained in measuring these angles corresponds however to a probable error of one degree for a single observation, so that reliance cannot be placed on the minutes of arc.

The following table collects the results obtained with one bipolar telephone[7] receiver B with two successive diaphragms, *i. e.*, diaphragm B and diaphragm 1. The first line in the table corresponds to the set of observations given in Fig. 4, where there was no load attached to the center of the diaphragm, the diameter Z_m of the motional-impedance circle was 81.25 ohms, the resonant frequency f_0 was 958 ~, the damping coefficient Δ, 245 hyperbolic radians per second, the force constant A, 5.49 megadynes per absampere, the equivalent mass m, 0.757 gm., the frictional or mechanical resistance r, 371 dynes per kine, the elastic constant s, 25.75 megadynes per cm. At the frequency f', of 1,013 ~, the angle $\beta_2{}^0$ was 46° 20′, and at 958 ~, $\beta_1{}^0$ was inferred to be 36° 38′.

TABLE I.

Effect of Diminishing Resonant Frequency on $\beta_1°$ and $\beta_2°$.

Test No.	Tel. Diaph.	Load Gm.	Z_m Ohms.	f_0 ~.	Δ $\frac{\text{hyps}}{\text{sec.}}$.	A $\frac{\text{dynes}}{\text{absamp.}}$. 10^6.	m Gm.	r $\frac{\text{dynes}}{\text{kine}}$.	s $\frac{\text{dynes}}{\text{cm.}}$. 10^6.	β_1.	β_2.	At f' ~.	$\beta_1 + \beta_2$.
1	B	0	81.25	958	245	5.49	0.757	371	25.75	36° 38′	46° 20′	1,013	82° 58′
2	B	0.6	97.5	761.4	169	7.75	1.32	616	41.5	29° 52′	46° 56′	811	76° 48′
3	B	0.6	97.5	796.5	173	6.69	1.33	459	33.3	25° 17′	53° 09′	850	78° 26′
4	B	0.73	92.5	794.5	141	7.18	1.95	551	48.6	24° 54′	51° 42′	845	76° 36′
5	B	1.2	102.5	680	100	7.07	2.44	487	44.6	19° 53′	52° 17′	732	72° 10′
6	1	0	17.6	1,100	261	5.36	3.08	1,608	148	57° 44′	28° 54′	1,132	86° 38′

Note: In the case of Test 2, the load of 0.6 gm. was applied to the diaphragm at its center; whereas in the case of Test 3 it was applied at a point 1 cm. off the center.

The successive series of observations 2, 4, and 5 were obtained by attaching increasing loads to the diaphragm, so as to lower the

[7] The details of this receiver are given in the paper of bibliography No. 10.

resonant frequency f_0. In the case of test No. 3, the load, a small copper disk, about 1 cm. in diameter, was intentionally placed on the diaphragm excentrically, *i. e.,* at a distance of 1 cm. off center. It will be seen from the table that as the resonant frequency f_0 was lowered, and with it f', the magnitude of $\beta_1{}^0$ was considerably reduced but $\beta_2{}^0$ was, if anything, slightly increased. The sum $\beta_1{}^0 + \beta_2{}^0$ between $f_0 = 680 \sim$ and $f_0 = 958 \sim$ has increased from about 72° to 83°; while $\beta_1{}^0$ has increased from 20° to 37°.

The inference to be drawn from this series of tests is that $\beta_1{}^0$ and $\beta_2{}^0$ are, in general, unequal. The angle $\beta_1{}^0$ increases with the frequency, but $\beta_2{}^0$ is apparently more nearly constant. A reason which suggests itself for this relation is that the lag $\beta_1{}^0$, between flux and current, is due not only to hysteresis but also to the eddy currents of skin effect. Owing to hysteresis and skin effect in the steel cores of the telephone electromagnet, the resultant flux lags behind the exciting current to an extent $\beta_1{}^0$ which depends upon the impressed frequency and may rise theoretically to 45° at relatively high frequencies, owing to skin effect alone. In the case of $\beta_2{}^0$, however, this is a lag between vibrational velocity of the diaphragm and the C.E.M.F. thereby produced. An oscillatory change in length of air-gap may set up hysteretic and eddy-current retardation in the flux oscillation thereby generated, but the skin effect should perhaps be less than when the flux oscillation is generated from an external magnetizing coil.

In order to ascertain the effect of an increased air-gap on the angles $\beta_1{}^0$ and $\beta_2{}^0$, ring washers of pasteboard, of successively increasing thickness, were inserted under the diaphragm, between it and the clamping surface of the receiver. Starting with a clearance between poles and diaphragm, of 0.32 mm. this was increased up to about 1 mm. with the results as shown in the following table, the

TABLE II.

EFFECT OF INCREASING AIR-GAP ON β_1 AND β_2.

Test No.	Tel. Diaph.	Clearance Mm.	D Ohms.	f_0 $\sim$.	Δ $\frac{\text{hyps}}{\text{sec.}}$.	A $\frac{\text{dynes}}{\text{absamp.}}$. $\times 10^6$.	m Gm.	r $\frac{\text{dynes}}{\text{kine}}$.	s $\frac{\text{dynes}}{\text{cm.}}$. $\times 10^6$.	$\beta_1{}^0$.	$\beta_2{}^0$.	At f' $\sim$.	$\beta_1{}^0 + \beta_2{}^0$.
1	*B*	0.32	92.5	794.5	141	7.18	1.95	551	48.6	24° 54′	51° 42′	845	76° 36′
2	*B*	0.70	25.6	764.3	76.4	3.92	3.93	600	90.6	36° 0′	48° 42′	783	84° 42
3	*B*	1.08	9.9	770.6	61.9	2.14	3.76	465	88.5	32° 54′	50° 24′	791	83° 18′

load attached to the center of the diaphragm being 0.73 gm. in each case.

It appears from this table that the increase in air-gap greatly diminished the force-factor A and the amplitude of vibration, which is proportional to the diameter D of the impedance circle. The equivalent mass and the elastic constant are both increased. It appears that β_2^0 has undergone but little change; whereas β_1^0 has distinctly increased.

The inference to be drawn from Table I. and Table II. collectively, is that β_2^0 seems to be nearly constant for a given receiver; but that β_1^0 is affected both by the air-gap length and the impressed frequency. Thus there seems to be no close connection between β_1^0 and β_2^0. In the first five cases of Table I., and in all the cases of Table II., the angle β_2^0 exceeds β_1^0; but this is not necessarily true in all cases. In test 6 of Table I., β_2^0 is considerably less than β_1^0. This case refers to another receiver and diaphragm. In the particular instrument investigated by Kennelly and Pierce[8] in 1912, the angles β_1^0 and β_2^0 happened to be nearly equal.

A number of tests were made with a series of different thicknesses of diaphragm in one and the same receiver. The results showed that the angles β_1^0 and β_2^0 were different with different diaphragms; but the quantitative relations have not yet been ascertained.

2. Investigation of Reëntrant and Distorted Circle Diagrams.

The engineering research department of the Western Electric Co., when examining some motional-impedance diagrams in 1913, seem first to have discovered cases of distorted and reëntrant circles. Such cases presented themselves in the course of the M. I. T. researches in 1915. Distorted diagrams of this type appear in Figs. 5 to 9 and 11 to 17 of this paper.

These distorted circle diagrams presented themselves at first in a small percentage of the cases of telephone receivers tested in the M. I. T. researches. When first encountered in these, they were regarded as curiosities of unknown origin, and were set aside. At

[8] Bibliography, 7.

a later period, they were taken up for investigation, since marked abnormalities of such a type adversely affect the circle-diagram method of analyzing telephone receivers. For a long time, the

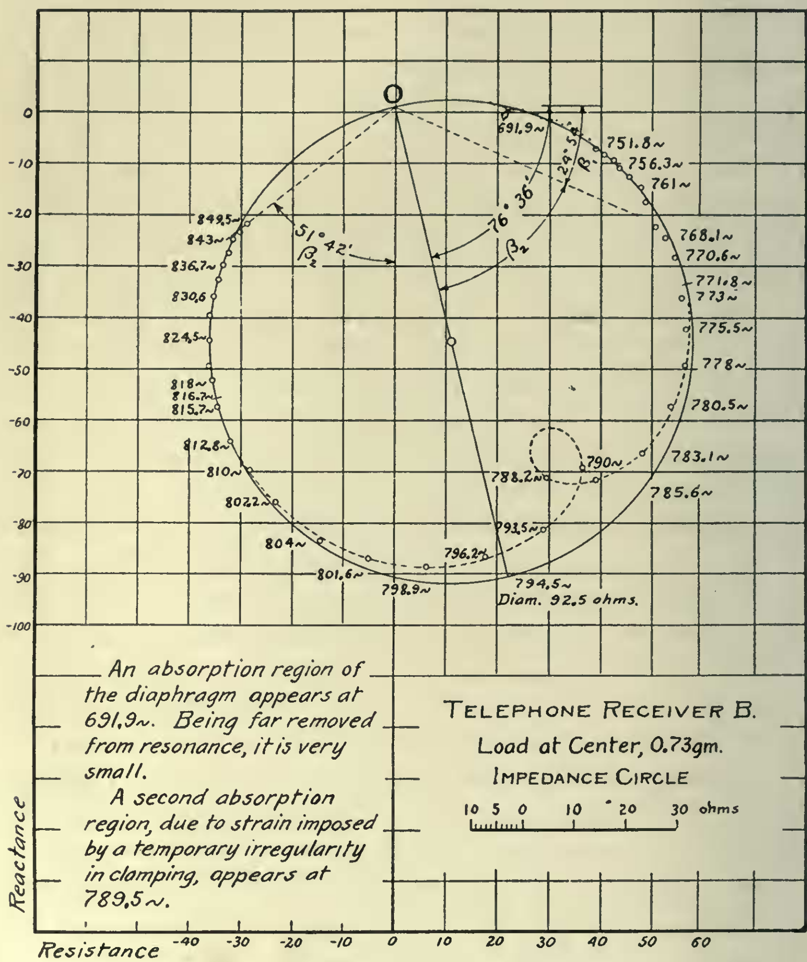

FIG. 5. Distorted Motional-Impedance Circle. Small Distortion, Rising on the right.

cause of these abnormalities baffled enquiry; but finally their origin was apparently brought to light, and it also became possible to produce them artificially, at will.

Fig. 4, already referred to in connection with the depression angles β_1^0 and β_2^0, presents a smooth motional-impedance circle, all the observed points falling nicely upon its circumference. Nevertheless, there is reason to believe that this circle contains a small inner loop distortion between the origin o and the lowest indicated frequency of 857 ~. No measurements were made in this case below 857 ~; but it is probable that, had they been made, the distortion loop would have been too small to notice. The central amplitudes of vibration were also measured by the explorer in the case of Fig. 4, and from these the vibrational velocities $\dot{x}$ of the diaphragm were computed. They lie closely to the inner circle indicated in the figure. This shows, moreover, as has been pointed out in earlier publications, that the motional-impedance circle may be regarded as a velocity circle, taken to a suitable scale, disregarding the phase lag β_2^0.

When the diaphragm of the receiver *B*, considered in Fig. 4, was loaded at the center by a small copper washer, about 1 cm. in diameter and weighing 0.73 gm., a repetition of the test gave the diagram shown in Fig. 5, the analysis of which appears in Table I. This diagram shows two internal loops or abnormalities, one a little loop near 691.9 ~, well defined however by numerous observations, and the other a larger loop near 789.5 ~. The latter proved to be a temporary visitor, and since it did not appear in subsequent tests. it may be left out of consideration here. It suffices, therefore, to notice that the loop at 691.9 ~ had a length of about 2.5 ohms, and occurs in the circle at an angular distance of about 30° from o, the origin of the circle. The resonant frequency of the loaded diaphragm as a whole was apparently 794.5 ~.

The load on the diaphragm was then increased to a total of 0.975 gm. This had the effect of bringing the resonant frequency down to 699.4 ~; or close to the frequency at which the abnormality (at 691.9 ~) had appeared. The result of the test under this condition is shown in Fig. 6. The distortion loop is central at 697.2 ~, and has a length of 42.5 ohms on the motional-impedance scale. It is evident that when the diaphragm is brought nearly into resonance with the frequency of the distortion loop, the magnitude of the loop is greatly enlarged. By drawing the circumference of the circle as it would appear in the absence of distortion, and marking off thereon the computed positions of the various observed fre-

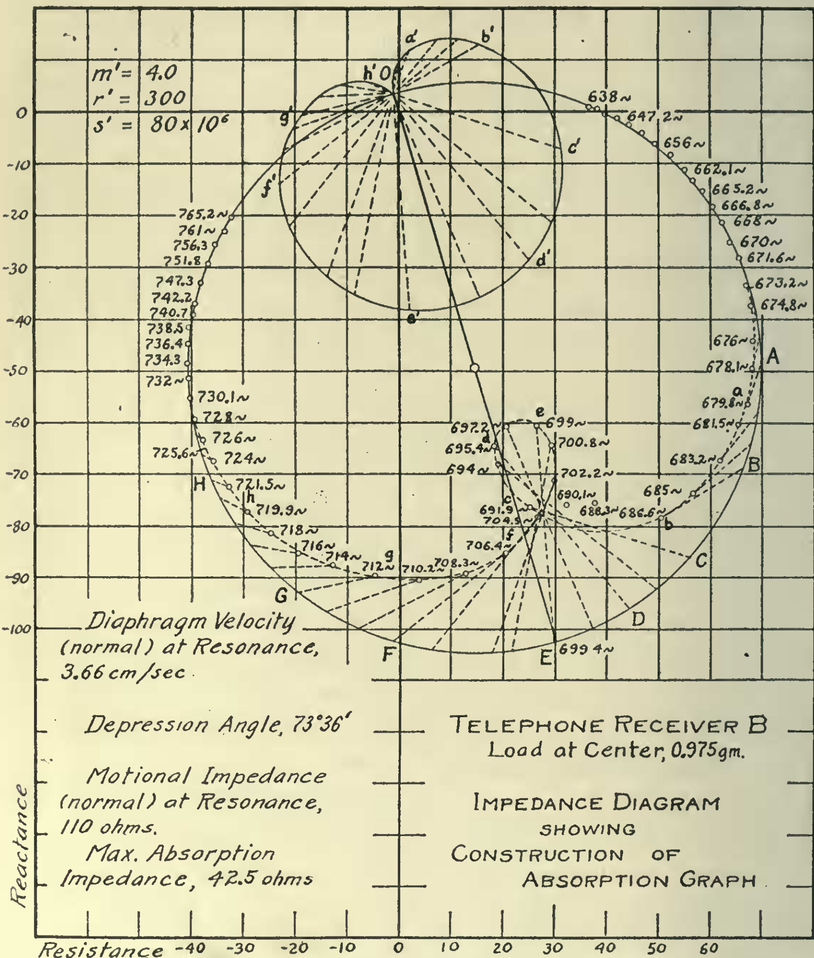

FIG. 6. Distorted Motional-Impedance Circle. Distortion Nearly Central on Main Diameter.

quencies, it was noticed that the chords, or vector differences, between the distorted and undistorted points gave rise to an approximate circular locus, when referred to the origin. This showed that, at least to a first approximation, the distortion consisted of a negative or absorption circle, of the same general character as the main impedance circle, but which is swept over much more rapidly. The constants A', m', r' and s' of this absorption circle were capable of being roughly determined.

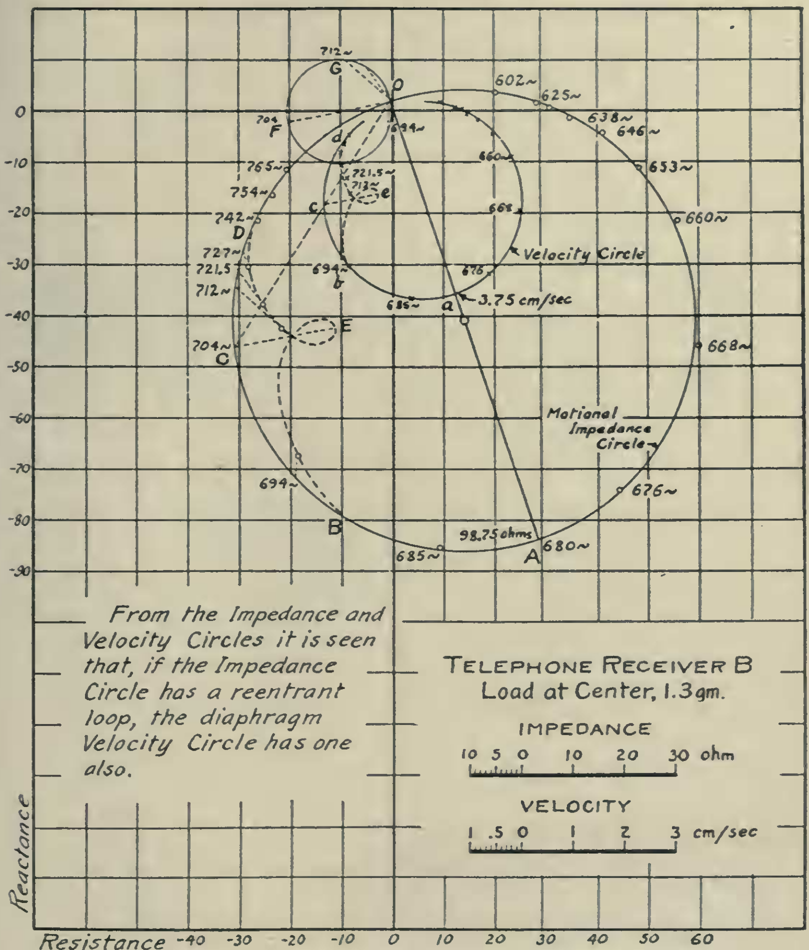

FIG. 7. Distorted Impedance and Velocity Circles. Distortion Loop Setting in the Left.

By still further increasing the load on the diaphragm to 1.3 gm., and thus bringing its resonant frequency to 680 ~, or below the frequency of the distortion, the next test, indicated in Fig. 7, showed that the distortion loop, central at 704 ~, had moved over to the left hand side of the diameter *OA*, and had diminished to

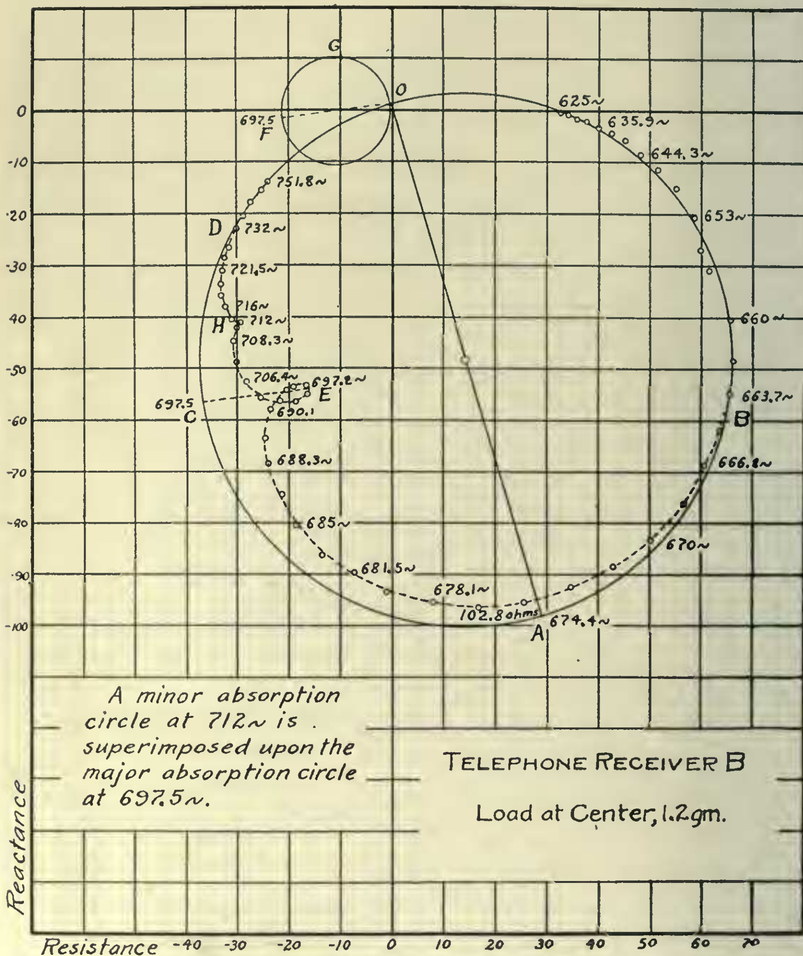

FIG. 8. Doubly Distorted Motional-Impedance Circle.

about 17 ohms of departure *CE*, from the main circle. The central amplitudes of the diaphragm's vibration were again measured in this case, and from them the inner circle of vibrational velocity *O abcd* was deduced. This also shows the distortion at *e*. The corresponding approximate motional-impedance distortion circle is marked at *OGF,* at an angle lagging more than 90° behind the diameter *OA*.

On reducing the diaphragm load to 1.2 gm., the distortion loop in Fig. 8 was enlarged to 20.5 ohms at *CE;* and the distortion at 697.5 ~ is brought slightly nearer to the bottom of the circle. The deduced distortion circle *OGF,* is also brought to a lag of somewhat more than 90° behind the diameter *OA*. Incidentally a small new and transient distortion appears at *H*.

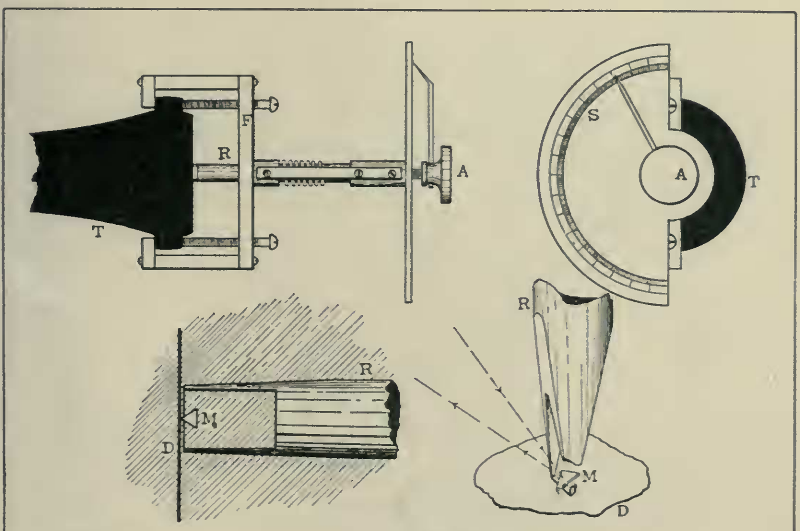

FIG. 9. Amplitude Measurer.

Summing up the disclosures of the last few figures, it appears that one and the same distortional disturbance in a diaphragm, resident near 700 ~, by suitably diminishing the resonant frequency of the diaphragm in successive steps, was made to appear, first as a small loop near the origin on the right-hand side, then as a greatly magnified loop near the diameter, and finally passing off as a small loop near the origin on the left-hand side. The deviations from the main circle are only approximately represented by absorption circles. Moreover, the angle *COF,* Fig. 7, is approximately equal to the angle *COA*.

An outline theory of the absorption graph is offered in Appendix II.

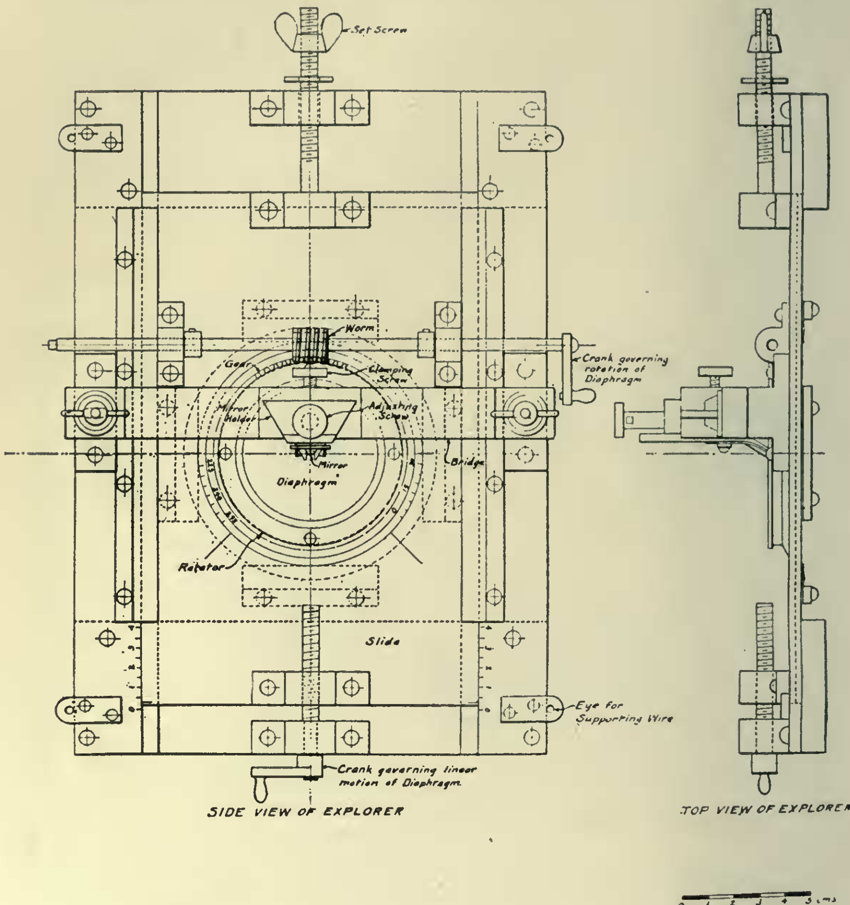

Fig. 10.

It was noticed, after a time, that whenever the distortion near 700 ∼ manifested itself, the amplitude measurer of Fig. 9 was mounted on the receiver. This particular form of amplitude measurer was described in an earlier publication. This led to the suspicion that the clamping screws in the brass frame *F* might be responsible for these distortions of the impedance circle. On actual trial, the removal of the amplitude measurer and its clamping frame from the receiver, removed the distortion from the impedance circle. It thus became evident that the application of clamping pressure to the composition cap of the telephone receiver, warped it slightly, and

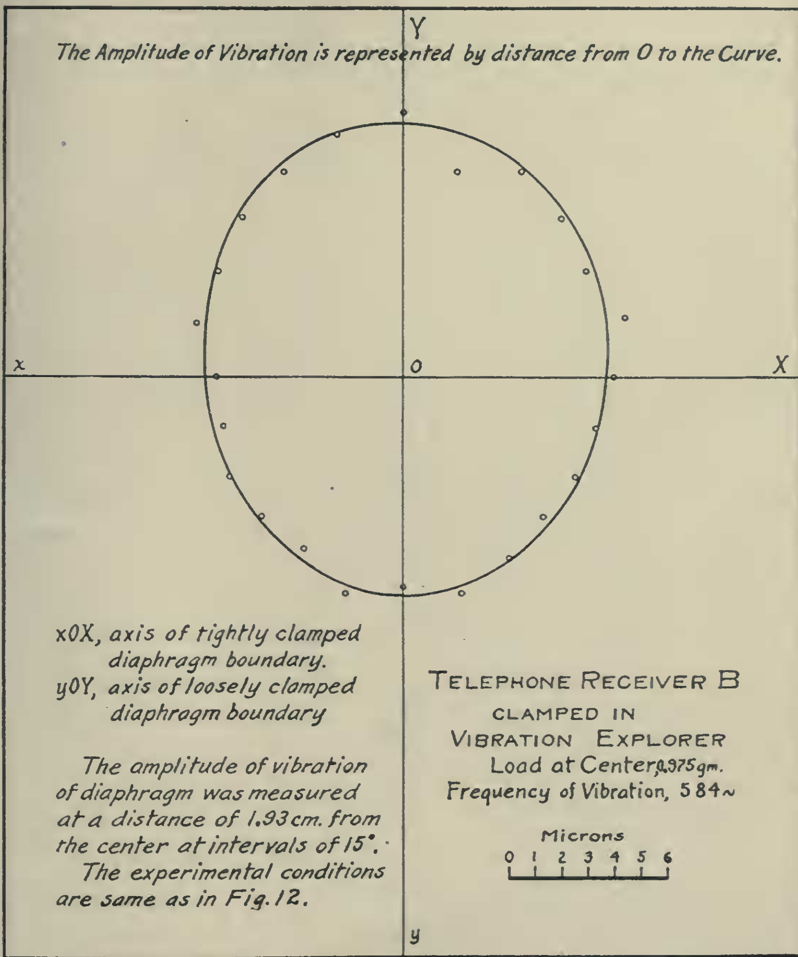

FIG. 11. Amplitudes of Vibration around Imperfectly Clamped Diaphragm.

interfered with the uniformity of boundary vibration around the clamping circle. This also indicated the importance of employing metallic clamping rings around the cap, or otherwise ensuring that

[9] Bibliography, Kennelly and Affel, Fig. 10.

the clamping of the diaphragm is unchanged when the amplitude measurer is applied.

In order to investigate the matter further, the diaphragm *B* of the receiver was mounted in the vibration explorer Fig. 10, described in a preceding paper.[10] It may be seen that the diaphragm is here supported under a clamping ring, which is attached to the main frame by four machine screws. Two of these screws, diametrically opposite each other, were removed, leaving the diaphragm clamped tightly under opposite points only, thus simulating the effects of the clamps of the amplitude explorer in Fig. 9. The diaphragm had a central load of 0.975 gm., and the same receiver *B* was screwed into the explorer to actuate it. The impressed frequency was maintained at 584 ∼, and with an alternating-current strength of 2.26 milliamperes rms. The amplitude of vibration under these conditions was measured at various angular positions 15° apart, at uniform radial distances, 1.93 cm. from the center, the clamping-ring diameter being 5.24 cm. The results obtained are shown geometrically in Fig. 11. Here the axis of the tightly clamped boundary is horizontal, and the axis of the loosely clamped boundary where the screws were removed, is vertical. It will be observed that the average amplitude in the latter axis is about 9 microns; while in the former it is about 7.6 microns; so that the mean amplitude along the loosely clamped diameter is some 18 per cent. more than that along the tightly clamped diameter, with intermediate values in intermediate directions. This indicates the importance of securing uniformly tight clamping around the boundary of a telephone diaphragm.

The motional-impedance diagram for this case is shown in Fig. 12. No localized distortion loop is visible; but there is a general shrinking of impedance, and therefore of diaphragm velocity, over a considerable range of the diagram (559 ∼ to 618 ∼). No distortion loop was obtained at any time in the vibration-explorer tests, as though no definite absorption frequency was brought about; but there was a fairly proportional degree of absorption over a wide range of impressed frequency.

[10] Bibliography No. 9, Kennelly and Taylor.

The inference from the preceding results was that a distortion loop was due to the presence of local and loosely clamped diaphragm boundary areas, having a natural frequency independent of the main

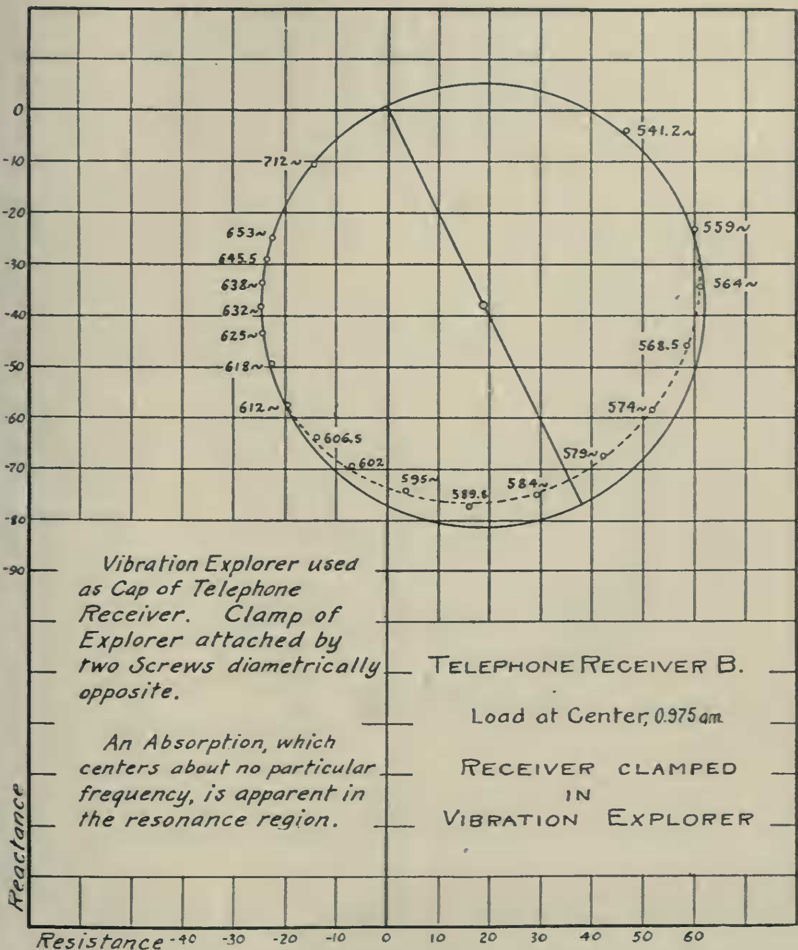

FIG. 12. Distorted Impedance Circle with Unlocalized Distortion.

diaphragm, and having constants *r, m,* and *s* of their own. The local areas received their vibrational energy from the main diaphragm. According to this view, it would only be necessary to attach a local vibrational system, with its own *r, m,* and *s* to a properly clamped diaphragm, in order to simulate the localized distortional behavior of an irregularly clamped diaphragm.

With this object in view, a small piece of bent hard copper strip was fastened by sealing wax to the center of the diaphragm, as shown in Fig. 13. The weight of this spring was 0.6 gm. in all, of which the free portion weighed only 0.2 gm. The free period

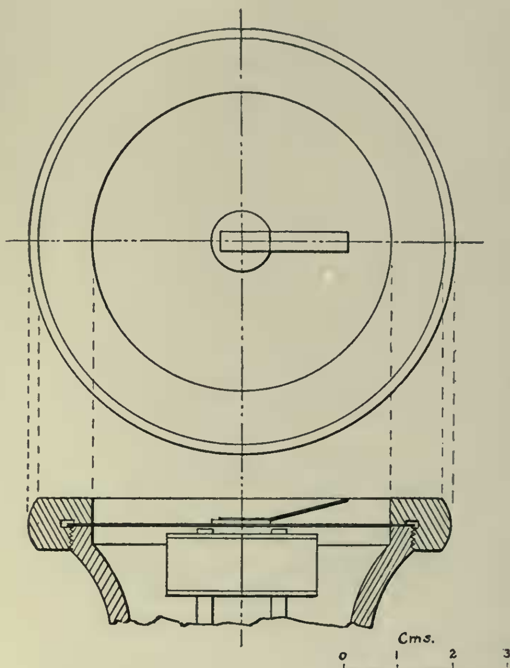

FIG. 13. Plan and Longitudinal Section of the Test Receiver with Secondary Vibrational System Attached to Center of Diaphragm.

of this spring, when mounted on the diaphragm, was adjusted, by trial, to approximately 750 ~, which is nearly the same as the diaphragm thus loaded. Fig. 14 shows the motional-impedance diagram of receiver *B* with the diaphragm and its spring load. It will be observed that between 660 ~ and 866 ~, the diagram forms a large reëntrant loop, and the actual amplitude, at 753 ~, is only about 4 per cent. of the inferred undistorted diameter *OA*. It is evident that, in this case, the form of the diagram is completely changed, there being now two maximum motional-impedances, one near 676 ~, and the other near 840 ~. Nearly midway between them (753 ~), the motional impedance almost vanishes at *OB*.

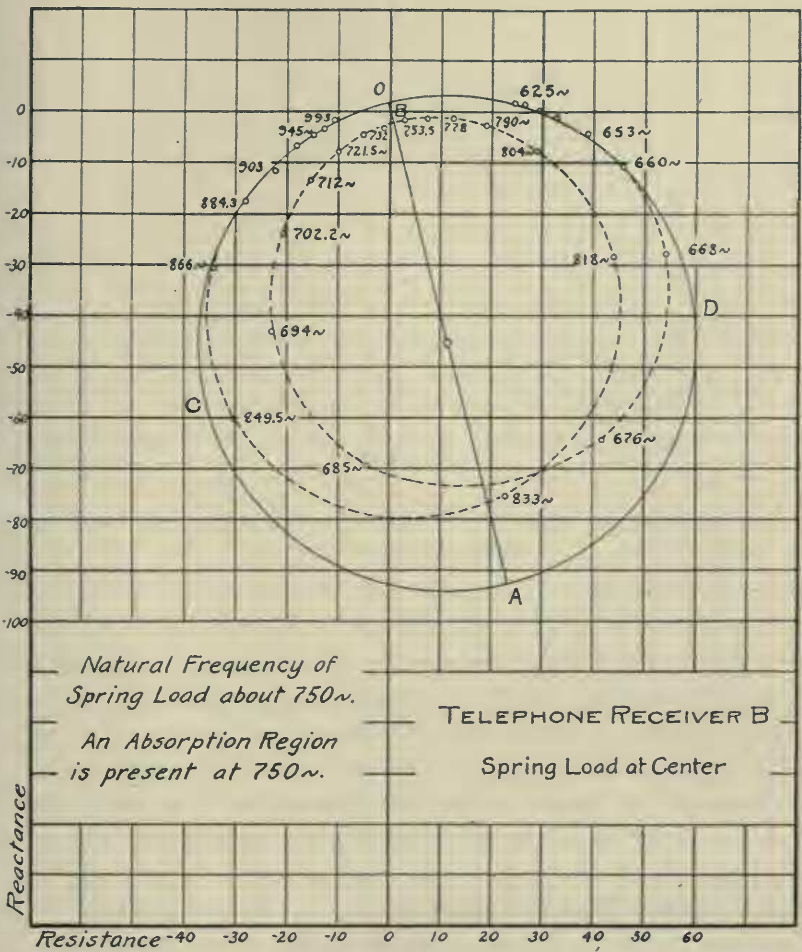

FIG. 14. Distorted Motional-Impedance Diagram. Large Distortion Loop.

The amplitudes of vibration of the diaphragm, as deduced from the motional-impedance diagram of Fig. 14, are shown in Fig. 15 with amplitude ordinates, and abscissas in impressed frequency. It will be seen that the amplitude almost vanishes at 753 ~, which is approximately the natural frequency of the loaded diaphragm obtained from the undistorted circle *OCAD* of Fig. 14. The curve of Fig. 15 has two sharp resonance peaks, whereas the inferred amplitude curve of the diaphragm, without abnormality, has, as usual, only one, *ABCDE*. It was noticed during the test represented in

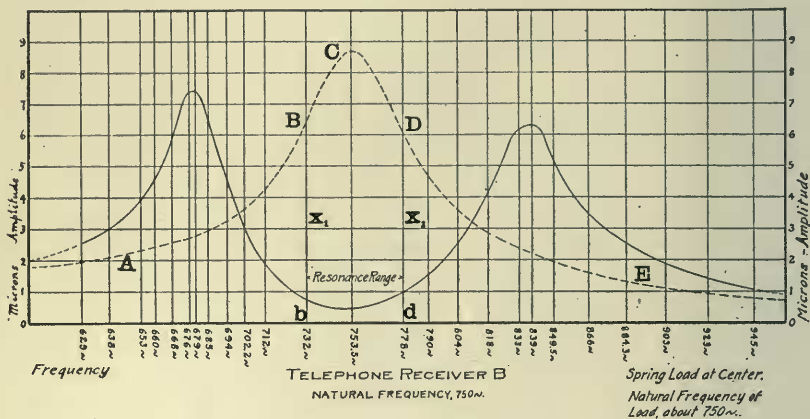

FIG. 15. Relative Amplitudes of Diaphragm Vibration with Spring Attached.

Fig. 14, that the receiver gave practically no sound at 753 ~; but gave loud sounds for frequencies slightly removed on either side of this. This peculiar property of a spring-loaded diaphragm to be silent at a certain selected frequency, but to sound loudly at a small departure therefrom on either side, may have practical applications.

The natural frequency of the spring load was then altered to about 913 ~, leaving the natural frequency of the diaphragm at 712 ~, a little below its preceding value. The effect of this change on the motional-impedance diagram is shown in Fig. 16. Here the distortion loop is reduced in diameter nearly one half, and is located much nearer to the origin on the left-hand side of the impedance circle.

By lowering slightly the natural frequency of the diaphragm to about 698 ~, leaving the natural frequency of the spring load unaltered, the distortion loop in Fig. 17 is brought still nearer to the origin *O*, and its dimensions further diminished.

When two independently clamped telephone diaphragms were mounted, one below the other, in parallel planes, the upper supported in the vibration explorer, the lower in the receiver B, and

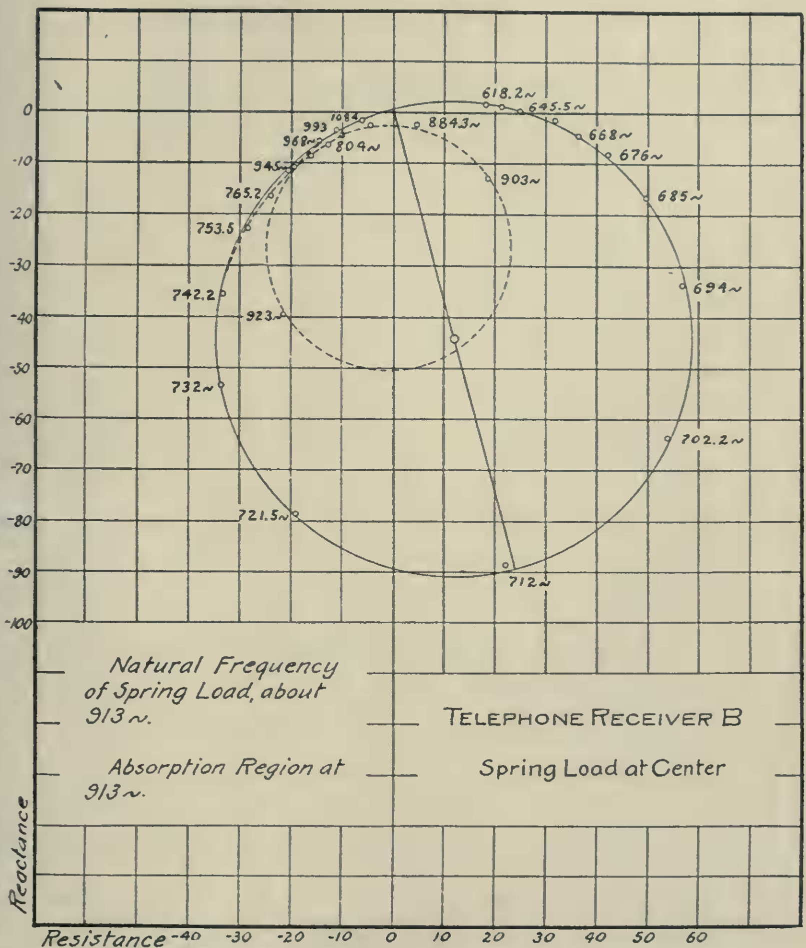

FIG. 16. Distorted Impedance Circle. Spring Load out of Tune with Diaphragm.

both connected rigidly, between their centers, by an aluminum bar 6 cm. long, and 2 mm. × 2 mm. in section, the whole system gave an undistorted motional-impedance circle, corresponding to the natural frequency and other constants of the composite single system. The inference seems therefore to be warranted, that any vibratory

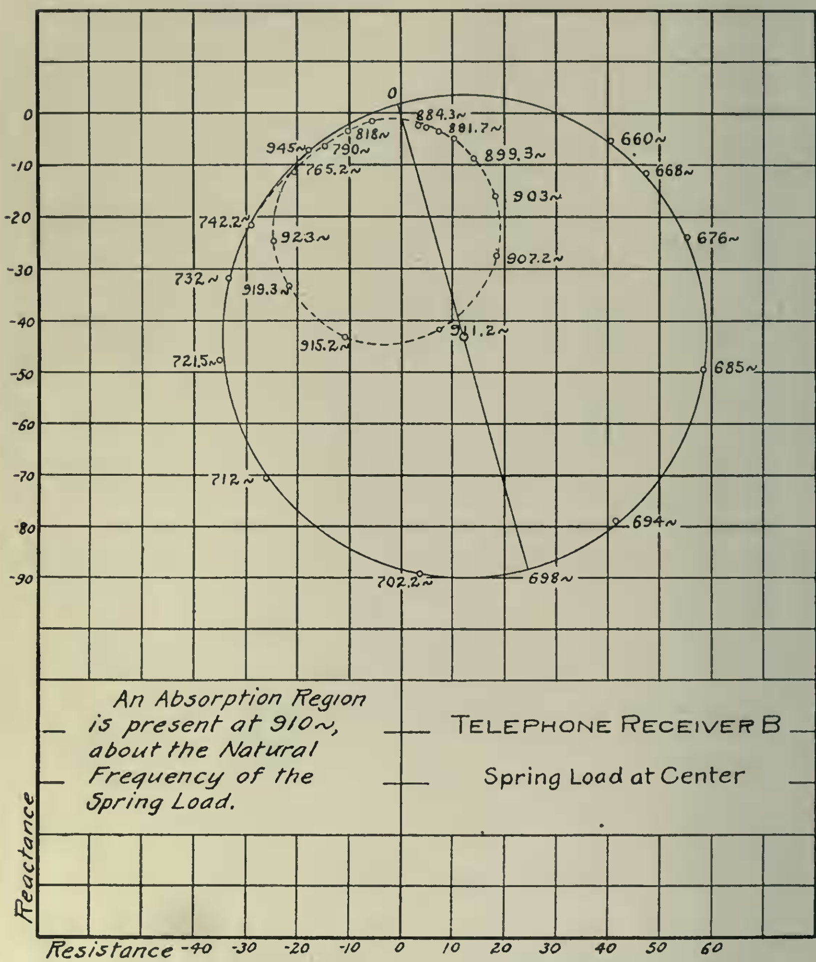

FIG. 17. Distorted Impedance Circle. Spring Load Further out of Tune with Diaphragm.

system including diaphragms properly clamped around their edges; but so connected as to possess only a single free period, will be unable to produce a distorted motional-impedance circle.

Torsion-Pendulum Model for Illustrating Motional Velocity Phenomena.

A psychological obstacle to the use of the motional-velocity circle conceptions, in their abstract quality, and remoteness from concrete apprehension. Thus, in the case of the telephone receiver, its motional-velocity circle is obtained through the medium of the motional-impedance circle, as determined from electrical measure-

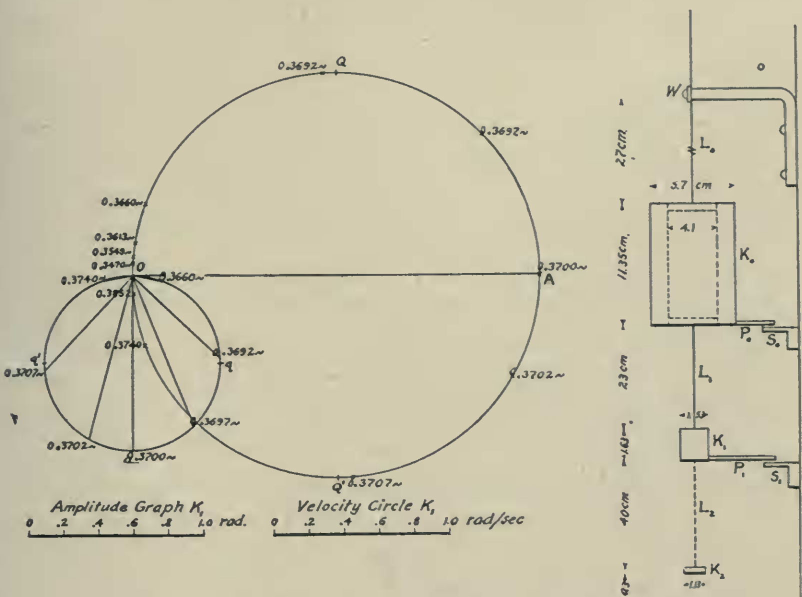

Fig. 18. Multiple Coupled Torsion Pendulum Model.

ments. It is therefore a great advantage to be able to construct a motional-velocity circle from direct observations on a simple dynamical model.

A useful and very simple dynamical model for illustrating the conditions of diaphragm vibration and the resulting motional-impedance circle has been designed and constructed as indicated in Fig. 18. It consists of a hollow brass cylinder K_0 which, in the particular model used, has a mass of 1,200 gm., a radius of gyration of 2.48 cm., and a moment of inertia of 7,470 gm.–cm.^{2}. This is suspended by a brass wire of diameter 0.76 mm., of a length adjustable, by means of a clamping screw w, between 10 and 40 cm., with a corresponding oscillation frequency range of 0.6 to 0.3 ~. The logarithmic decrement being very small, it oscillates about the suspension-wire axis with but little diminution of amplitude for several minutes. In the model used, the time constant, or the time of fall to $1/\epsilon$th amplitude, is 216 seconds. This driving cylinder takes the place of the A.C. generator in the case of the telephone. The smaller solid brass cylinder K_1 has a mass of 26.8 gm. and a moment of inertia of 8.4 gm.–cm.^{2}. It is suspended from the driving cylinder by a smaller wire of copper, having a length usually kept constant at 23 cm., and of 0.13 mm. diameter. This driven cylinder corresponds to the telephone diaphragm, and performs oscillations of the period impressed on it by K_0. The driving cylinder K_0 is so much larger than the driven cylinder K_1, that the reaction of the latter is insignificant. With K_0 and K_1 in action, all the dynamical phenomena of the telephone diaphragm and its velocity circle can be observed, the frequency impressed by K_0 being adjusted by successive steps through a considerable range, by shortening up the main suspension wire L_0. As the impressed frequency overtakes and passes the natural frequency of K_1, with its suspension L_1, the phenomena in the vicinity of resonance are reproduced. The K_1 system has its m, r, and s, in substantially the same manner as the oscillographic systems described in Appendix I.

Technique of Model.—In operating the model, the cylinder K_0 is first set by hand in torsional oscillation about the suspension-wire axis, with the lowest frequency of longest suspension L_0, and with as little side swing as possible. The initial angular amplitude of K_0 may be made 90° or more. After a few oscillations, the coupled pendulum system settles down to a substantially steady state, the oscillations of K_1 having the same frequency as those of K_0. The oscillations are allowed to subside naturally under the damping constant ($\Delta = 0.00462$ hyps. per second) until a convenient standard amplitude is reached, as is indicated by a pointer P_0, upon a suitably supported angular scale S_0. When this happens, the eye of the observer at O can observe also the angular amplitude of K_1 as well as the angular phase-difference of the two elongations at P_0S_0 and

P_1S_1. The decay of amplitude is so slow, that these conditions repeat themselves very closely for several oscillations above and below the standard amplitude of K_0; so that the observations can be repeated at several successive oscillations for an average.

The oscillation frequency of K_0 is then increased in small successive steps, by shortening up the suspension L_0, and the above mentioned observations are repeated at each step. The amplitude of oscillation of K_1 increases rapidly as resonance is approached. In the model used, the resonant sharpness Λ is 252, but this can be controlled at will, by applying any motional resistance to K_1 which is substantially proportional to the velocity. Fig. 18 gives the angular-amplitude and angular-velocity circles for the model. It is seen that the semicircular range of resonant frequency, as computed from the circle diagram, is between 0.3692 $\sim$ at ω_1 and 0.3707 $\sim$ at ω_2. For impressed frequencies below this range, the oscillation of K_1 comes nearly into cophase with K_0. On the other hand, at impressed frequencies above this range, the amplitude of K_1 comes nearly into opposite phase with K_0. At resonance, the oscillation of K_1 is in quadrature with the amplitude of K_0; or the angular velocity of K_1 will be in cophase OA with the vector torsional force or vibromotive force (V.M.F.) exerted by the wire on K_1. This V.M.F. is proportional to the angular displacement between the ends of L_1, and the observations obtained must be corrected to constant maximum cyclic V.M.F.

A student working with the model in the above described manner, can acquire a concrete conception of a motional-velocity circle, based upon direct observations of oscillations executed so leisurely that they are easily observed directly by the eye, without the use of reflecting mirrors or of electrical apparatus. Moreover the oscillations are sufficiently large to be perceived directly by a large class. When K_1 oscillates in air, the motional resistance r seems to increase somewhat with the amplitude. When K_1 was allowed to oscillate in water, the motional resistance was found to be more nearly constant.

When it is desired to study the phenomena of absorption, a secondary torsion pendulum L_2K_2 is attached to K_1. It is then convenient to adjust the natural frequency of the secondary pendulum

K_2 into approximate coincidence with that of K_1. Under these conditions, the phenomena of absorption, at or near resonance, can be readily observed. It has been possible in this manner to check the causes and essential characteristics of telephone-diaphragm absorption.

Absorbing Influence of the Amplitude Measurer on the Vibration of a Diaphragm.

It was observed in the course of the preceding tests, in which the amplitude measurer was successively on and off the receiver, that the application of the device, apart from the warping effect of its clamps, slightly diminished the diameter of the impedance circle. In one case, this diameter, without the explorer, was 100.6 ohms, and with the explorer 92.5, all other conditions remaining unchanged. In other words, the application of the amplitude measurer reduced the vibrational velocity and vibrational amplitude about 8 per cent., without appreciably affecting the other constants of the instrument. This shows that when precision is needed, the motional-impedance circle should be taken with the amplitude measurer both on and off successively. The difference between the two motional-impedance diameters will indicate what correction should be applied to the measured amplitudes.

In conclusion, the authors desire to express their acknowledgments to Professor C. A. Adams and Mr. A. A. Prior, for their collaboration in the analysis of an oscillograph; also to Dr. G. A. Campbell for valuable criticisms and suggestions on the MSS.

APPENDIX I.

Outline Theory of the Bifilar Oscillograph and Duddell Vibration Galvanometer.[11]

It is assumed that the apparatus consists of a bifilar vertical suspension, of adjustable tension, part of which suspension vibrates in a fairly uniform magnetic field. The two vertical wires of the

[11] This theory is substantially the same as that developed in the Kennelly and Affel paper (Bibliography, 10), with respect to vibrating diaphragms, replacing translatory forces by corresponding couples.

suspension carry the testing current, and are connected mechanically by a small mirror, which optically serves to indicate the angular displacement of the bifilar system at the mirror. It is further assumed that the restoring torque is $s\theta$ dyne-perpendicular-cm.,[12] proportional to the angular displacement θ radians; that the resisting torque dissipating the energy of motion is $r\dot{\theta}$, or is proportional to the angular velocity $\dot{\theta}$ radians per second; also that the inertia torque, resisting change of angular displacement, is $m\ddot{\theta}$, where m is the equivalent moment of inertia of the system at the mirror, and $\dot{\theta}$ is the angular acceleration in radians per sec.^{2}. The impressed displacing torque, or vibromotive torque (V.M.T.), is assumed to be simply harmonic of the type

$$f = I_m A \epsilon^{j\omega t} = iA, \quad \text{dyne perp. cm. } \angle, \quad (1)$$

where i is the complex instantaneous current passing through the suspension, with maximum cyclic value I_m absamperes. A is the torque constant of the instrument, in dyne perp. cm. per absampere, $j = \sqrt{-1}$, $\omega =$ the impressed angular velocity, and t is the time in seconds from the moment when the real component of i starts positively through zero towards its maximum cyclic value. The real component of (1) is the instantaneous torque. The equation of motion is

$$m\ddot{\theta} + r\dot{\theta} + s\theta = f, \quad \text{dyne perp. cm. } \angle, \quad (1)$$

whence, in the steady state, *i. e.*, neglecting the exponentially decaying transient term,

$$\dot{\theta} = \frac{f}{r + j\left(m\omega - \frac{s}{\omega}\right)} = \frac{f}{z}, \qquad \frac{\text{radians}}{\text{sec.}} \angle. \quad (3)$$

Here z is the mechanical impedance of the vibratory system. In the ordinary bifilar oscillograph, none of the four constants A, m, r and s is supposed to change, except through accidental changes of temperature. In a vibration galvanometer, however, the tuning of the vibratory system imposes changes in the impedance z, and in its

[12] In a torque τ, dyne-perp.-cm., the force f_1 dynes is assumed to act perpendicularly to the radius arm 1 cm., at which it is applied. A torque is therefore not properly expressible as dyne-cm., but as dyne perpendicular cm.; or dyne $\perp$ cm.

components, especially in the elastic constant s.

From 3, we have

$$\theta = \frac{\dot{\theta}}{j\omega} = \frac{f}{j\omega\left\{r + j\left(m\omega - \frac{s}{\omega}\right)\right\}}, \quad \text{radians} \angle \quad (4)$$

The instantaneous E.M.F. overcoming the counter E.M.F. of vibration is

$$e_x = A\dot{\theta} = \frac{Af}{z} = \frac{A^2 i}{z} = iZ, \quad \text{abvolts} \angle, \quad (5)$$

where Z is the motional-impedance of the instrument.

Hence, at resonance,

$$A\dot{\theta}_m = I_m Z_m, \quad \text{abvolts}, \quad (6)$$

and

$$A = \frac{I_m Z_m}{\dot{\theta}_m} = \frac{I_m Z_m}{\omega_0 \theta_m}, \quad \frac{\text{dyne perp. cm.}}{\text{absampere}}, \quad (7)$$

where I_m is the maximum cyclic value of the current in absamperes, Z_m is the maximum motional-impedance—which is reactanceless, or a simple resistance—and θ_m the observed maximum cyclic resonant angular displacement, in radians. The resonant impressed angular velocity at which this occurs is denoted by ω_0 radians per second.

At $\omega = \omega_0$ (4) becomes

$$\theta_m = \frac{AI_m}{\omega_0 r}, \quad \text{radians}, \quad (8)$$

whence

$$r = \frac{AI_m}{\theta_m \omega_0}, \quad \frac{\text{dyne perp. cm.}}{\text{radian per second}}. \quad (9)$$

From the motional-impedance circle of the instrument, as plotted from observations of impedance at different impressed frequencies, the decrement per second Δ, or the hyperbolic angular velocity of decay in amplitude, may be obtained, by taking half the difference between impressed angular velocities ω_1, ω_2 at the quadrantal points in the circle; or

$$\Delta = \frac{r}{2m} = \frac{\omega_2 - \omega_1}{2} = \pi(n_2 - n_1), \quad \text{hyps. per sec.}, \quad (10)$$

where n_1 and n_2 are the corresponding impressed frequencies; whence

$$m = \frac{r}{2\Delta} = \frac{r}{\omega_2 - \omega_1}, \qquad \text{gm.-cm.}^2. \quad (11)$$

At these quadrantal frequencies, the deflection amplitudes will be very nearly $\theta_m/\sqrt{2}$ radians. Finally, by observing the angular velocity ω_0 of resonance, when θ_m becomes a maximum, we obtain

$$\omega_0 = \sqrt{\frac{s}{m}}, \qquad \text{radians/sec.,} \quad (12)$$

whence

$$s = m\omega_0^2, \qquad \frac{\text{dyne perp. cm.}}{\text{radian}}. \quad (13)$$

Consequently, all four constants A, m, r and s can be found for any assigned adjustment of the vibration galvanometer, by measuring (a) its motional-impedance Z_m in a Rayleigh bridge, to a measured alternating current I_m maximum cyclic absamperes, (b) noting the deflection θ_m in radians, at resonance, on either side of the scale zero, (c) the resonant angular velocity ω_0 and (d) the impressed frequencies at the quadrantal points n_2, n_1 cycles per second.

Two additional checks on the above results can be obtained, if desired, (1) by passing a small measured continuous current I_s absamperes from a storage cell and measuring the steady deflection produced. If θ_s is the corresponding steady deflection obtained, in radians; then

$$s\theta_s = I_s A, \qquad \text{dyne perp. cm.,} \quad (14)$$

whence

$$s = \frac{I_s A}{\theta_s}, \qquad \frac{\text{dyne perp. cm.}}{\text{radian}}. \quad (15)$$

It should be noted, however, that the value of s, obtained in this continuous-current test, is found to differ slightly from that found by A.C. measurements. The latter are to be preferred when available. (2) By disturbing the vibratory system, and allowing it to oscillate freely to rest, according to the formula.

$$\frac{\theta_t}{\theta_0} = \epsilon^{-\Delta t}, \qquad \text{numeric,} \quad (16)$$

where θ_t is the oscillographically recorded amplitude, at a time t seconds after release, when the initial amplitude is θ_0 radians.

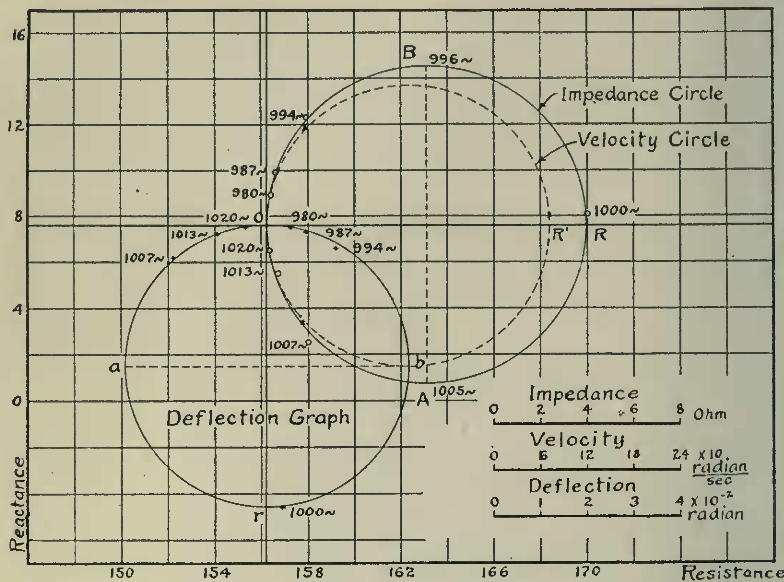

Observations

Freq. ~	Resist. ohm	React. ohm	Defl. rad.
980	156.3	8.95	0.0052
987	156.6	9.88	0.0087
994	157.9	12.38	0.0157
1000	170.0	8.46	0.0611
1007	158.0	2.53	0.0209
1013	156.7	5.48	0.0105
1020	156.3	6.44	0.0044

Max. Resonance Impedance, 13.8 ohms
Max. Resonance Deflection, 0.0611 rad.
Current Strength, $5.5 \cdot 10^{-4}$ amperes. r.m.s.
Quadrantal Points at 996~ and 1005~
Natural Frequency, 1000.5 ~.

Calculations

Current, Max. Cycl. Value, $7.78 \cdot 10^{-5}$ abs amp.
Max. Vib. Velocity, 383 rad/sec.
Log. Decrement per second, Δ, 28.3 hyps./sec.
A, Torque Const., 2804 $\frac{\text{dyne} \perp \text{cm}}{\text{abs amp}}$
m, Equiv. Moment of Inertia, $1.006 \cdot 10^{-5}$ gm-cm^2
r, Resistance Const., $5.697 \cdot 10^{-4}$ $\frac{\text{dyne} \perp \text{cm.}}{\text{rad/sec.}}$
s, Elastic Const., 397.5 $\frac{\text{dyne} \perp \text{cm.}}{\text{rad.}}$

DUDDELL VIBRATION GALVANOMETER.

FIG. 19. Motional-Impedance, Velocity and Deflectional Circles.

Fig. 19 shows two circular graphs starting from the common origin O, for the Duddell galvanometer used, as tuned to 1000 ~. The circle $OARB$ is the motional-impedance circle at impressed frequencies (obtained from a Vreeland oscillator and Rayleigh bridge), between 980 ~ and 1,020 ~. It will be observed that the maximum impedance of the instrument Z_m, at resonance, was the diametral resistance $OR = 13.8$ ohms, or 13.8×10^9 absohms. The R.M.S. current strength in the instrument was 0.55 milliampere $= 5.5 \times 10^{-5}$ absampere. The maximum cyclic current I_m was thus 7.78×10^{-5} absampere. At the impressed resonant frequency of 1,000.5 ~, the angular velocity would be $\omega_0 = 6{,}286$ rad./sec. Substituting in (7)

$$A = \frac{7.78 \times 10^{-5} \times 13.8 \times 10^9}{6.286 \times 10^3 \times 0.611 \times 10^{-1}} = \frac{107.4 \times 10^4}{3.83 \times 10^2}$$

$$= 2804 \frac{\text{dyne perp. cm.}}{\text{absampere}}.$$

The lower circle in Fig. 19, *Oa* and *b* shows the magnitudes of the deflections, each side of the scale zero, in radians of arc. The maximum observed deflection at $Or = 0.0611$ radian, was obtained, within the limits of experimental error, at the same frequency as the maximum resistance OR of the motional-impedance circle. Substituting the value of A just found in (9) we obtain

$$r = \frac{2.804 \times 10^3 \times 7.78 \times 10^{-5}}{0.611 \times 10^{-1} \times 6.286 \times 10^3} = \frac{21.82 \times 10^{-2}}{3.83 \times 10^2}$$

$$= 5.697 \times 10^{-4} \frac{\text{dyne perp. cm.}}{\text{rad. per sec.}}.$$

The maximum cyclic displacing torque was by (1)

$$7.78 \times 10^{-5} \times 2.804 \times 10^3 = 0.2182 \text{ dyne perp. cm.}$$

The quadrantal points B and A on the motional-impedance circle are at 996 ~ and 1,005 ~, making the damping constant $\Delta = 3.142 \times 9 = 28.3$; so that the oscillations of the instrument would naturally fall to $1/\epsilon$th, or to 36.8 per cent. of the initial amplitude, in a time constant of $1/28.3 = 0.0353$ second. Substituting this value of Δ in (11), we obtain

$$m = \frac{5.697 \times 10^{-4}}{56.6} = 1.006 \times 10^{-5} \text{ gm.-cm.}^2; \text{ or } \frac{\text{dynes}}{\text{rad. per sec.}^2}.$$

Finally from (13), we obtain

$$s = 1.006 \times 10^{-5} \times 6286^2 = 397.5 \, \frac{\text{dyne perp. cm.}}{\text{radian}}.$$

The reason for making the diameter Or of the deflection graph lag 90° behind the diameter OR of the impedance circle, and the diameter OR' of the velocity circle, is that according to (4), the phase of any displacement θ is 90° behind the corresponding velocity $\dot{\theta}$. Strictly speaking, while the velocity graph is a circle; the deflection graph is only approximately a circle, since in (4), the variable ω appears directly as a factor in the denominator. The angular velocity of maximum deflection ω_d is not the same as the resonant angular velocity ω_0, but is

$$\omega_d = \sqrt{\omega_0^2 - 2\Delta^2}, \qquad \frac{\text{radians}}{\text{sec.}}, \qquad (17)$$

while the angular velocity of free oscillations ω_f, in the presence of damping, lies between ω_d and ω_0; namely

$$\omega_f = \sqrt{\omega_0^2 - \Delta^2}, \qquad \frac{\text{radians}}{\text{sec.}}. \qquad (18)$$

In this case, taking $\omega_0 = 6{,}286.0$, $\omega_f = 6{,}286.06$ and $\omega_d = 6{,}286.13$; or the damping is so small, and the resonance is so sharp, that the difference between these three important and characteristic angular velocities is very small.

We may define the *sharpness* of *resonance,* or *sharpness* of *tuning* (inverted V),[13] in relation to the resonant and quadrantal angular velocities ω_0, ω_2 and ω_1 by the formula[13]

$$\Lambda = \frac{\omega_0}{\omega_2 - \omega_1} = \frac{\omega_0}{2\Delta} = \frac{n_0}{n_2 - n_1}, \qquad \text{numeric}, \qquad (19)$$

which in this case is $6{,}286/56.6 = 111.1$, a relatively high figure of merit in regard to tuning.[14] The reciprocal of Λ may perhaps be

[13] Suggested by Dr. R. L. Jones. Bibliography No. 8. The expression "sharpness of tuning" has also been suggested by Barton (bibliography, 4) with a different quantitative meaning.

[14] In the case of a certain experimental monopolar telephone receiver, tested by Kennelly and Pierce (bibliography, 7), the sharpness of resonance was found to be 161.2, the highest experimental value in electromagnetic apparatus yet observed in these researches.

called the *bluntness of resonance,* in this case 9.006×10^{-3}. The semicircular *range of resonance* may be expressed in angular velocity measure, as the range of angular velocity $\omega_2 - \omega_1$ between quadrantal points, or 2Δ, in this case 56.6 radians per second. The same range may be expressed also in frequency measure by $n_2 - n_1$, or the difference of frequencies at quadrantal points $= \Delta/\pi$, in this case 9 ~. All frequencies outside of these quadrantal points may be regarded as outside the semi-circular range of tuning. At the frequencies of these quadrantal points, n_2, n_1, the resonant kinetic energy manifestly falls to one half.

Referring to the dotted curve *ABCDE,* Fig. 15, of the undistorted amplitude of the diaphragm's vibration, the ordinates *Bb* and *Dd* indicate the amplitudes bounding the resonant range. The expressions defining these ordinates x_1 and x_2 are:

$$\frac{x_1}{x_0} = \frac{1}{\sqrt{2}} \cdot \frac{n_0}{n_1} \quad \text{and} \quad \frac{x_2}{x_0} = \frac{1}{\sqrt{2}} \cdot \frac{n_0}{n_2}, \qquad \text{numeric,} \quad (19a)$$

These ordinates are 6.35 and 6.0 microns, respectively, in Fig. 15. The resonant range is $778 - 732 = 46$ ~, and the resonant sharpness is thus $753.5/46 = 16.4$. It is thus possible to determine the sharpness and the range of resonance from a curve of amplitude against frequency, as well as from a circle diagram of velocity or of impedance.

The sharpness of resonance may also be defined by the acoustic interval or numerical ratio c between the quadrantal frequencies.

$$c = \frac{\omega_2}{\omega_1} = \frac{n_2}{n_1}, \qquad \text{numeric.} \quad (20)$$

In this case $c = 1.009$. We also have

$$\frac{\omega_0}{\omega_1} = \frac{\omega_2}{\omega_0} = \sqrt{c}, \qquad \text{numeric.} \quad (21)$$

This criterion c is connected with the resonant sharpness Λ by the relation

$$\Lambda = \frac{\sqrt{c}}{c - 1}, \qquad \text{numeric,} \quad (22)$$

since any pair of frequencies, lying on the velocity circle, at equal angles on opposite sides of the resonant diameter, have the resonant frequency as their geometric mean. The acoustic criterion c is, however, in general, less satisfactory than the resonant sharpness Λ; because the greater the resonant sharpness the greater becomes Λ but the smaller becomes c.

From an examination of Fig. 19, it is evident that, at resonance, the phase of the deflection or angular displacement of the mirror is just 90° behind the phase of the angular velocity, and of the current in the instrument. If OR represents the current phase; then, at resonance, Or is the phase of the mirror's maximum elongation. At impressed frequencies below 980 ∼, the phase of displacement in the deflection graph is almost exactly coincident with that of the current. On the other hand, at impressed frequencies above 1,020 ∼, the phase of displacement is almost exactly opposite to, or 180° removed from, that of the current.

An attempt was made to ascertain how the constants A, m, r and s of the Duddell instrument varied with different tuning and lengths of free suspension. It was found, however, that owing to some friction in the suspension pulley, the tension of the two wires did not equalize sufficiently to prevent the appearance of partial unifilar characteristics, which vitiated the results. Such departures from pure bifilarity would not, however, affect the above mentioned phase relations between displacement and current.

A similar set of measurements may be applied to an oscillograph. The normal alternating-current strength required to operate the oscillograph may, however, be greater than can conveniently be supplied through a Rayleigh bridge, as used for testing telephones or vibration galvanometers. In that case, a convenient technique is to supply a measured R.M.S. current from a Vreeland oscillator to the oscillograph vibrator, and observe the amplitude of the mirror's deflection thereby produced, on each side of the zero, reducing the same to radian measure from the geometry of the optical system. The angular velocity ω_0 radians per second, necessary for maximum resonance, has to be carefully observed, and at the same time the maximum resonant mirror deflection θ_m radians. This gives equations (8) and (12). The frequency is then gradually changed until the deflection is reduced in the ratio $1/\sqrt{2}$, the change being made first by raising the frequency slightly above resonance, and then lowering it. These measured angular velocities ω_2 and ω_1 correspond to the quadrantal points on the motional-impedance circle, and supply Δ by formula (10). Finally, the continuous-current strength, I_s abamperes, necessary to produce a steady mirror deflection θ_s radians, is measured as in (14). These four equations suffice to evaluate A, m, r and s for the instrument. An oscillographic natural decay curve, corresponding to (16), may also be taken as a check on the results.

The following are the results of a series of observations made on an experimental bifilar oscillograph[15] with two strips, each of active length 3.5 cm. in a magnetic field of approximately 16 kilogausses. The strips were of phosphor bronze, 0.366 mm. wide (15 mils), and 0.013 mm. thick (0.5 mil), each under a tension of approximately 30 gm. weight, spaced 1.5 mm. on centers, and having a mirror fastened to and across them, about 1 mm. $\times$ 0.5 mm., near the middle of their active length. The vibrator was air damped, *i. e.*, it did not work in oil.

$A = 3{,}750$ dyne perp. cm. per abampere,

$n_0 = 2{,}530.5 \sim$, $\omega_0 = 1.59 \times 10^4$ radians/sec.,

$m = 1.322 \times 10^{-5}$ gm.-cm.^{2},

$r = 2.78 \times 10^{-3}$ dyne perp. cm. per radian per sec.,

$s = 3{,}360$ dyne perp. cm. per radian,

$n_2 = 2{,}547 \sim$, $n_1 = 2{,}514 \sim$,

$\Delta = 103.7$ hyps. per sec.,

$\Lambda = 76.7$,

$n_2 - n_1 = 33 \sim$,

$\theta_s / \dot{I}_s = 1.115$ radians per abampere,

$I_m = 0.002$ absampere,

$Z_m = 5.075 \times 10^9$ absohms $= 5.075$ ohms.

By plotting the deduced angular velocities $\dot{\theta}$ at different impressed frequencies close to resonance, a fairly good circular locus was obtained. The diagram is the same as that of Fig. 19, except as to the scales of magnitude and numerical values.

[15] Bibliography, 11.

APPENDIX II.

Outline Theory of the Absorption Diagram.

The following provisional theory was arrived at by searching for a quantitative expression that would satisfy the impedance diagrams when distortion was present. It bears a close analogy to the theory of alternating-current coupled circuits in the steady state.

The equation for the ordinary motional-impedance circle, considered as representing a vibration velocity circle, and neglecting the depression angles $\beta_1{}^0$ and $\beta_2{}^0$ is[16]

$$\dot{x}_m = \frac{AI}{z} = \frac{F}{z} = \frac{F}{r + j\left(m\omega - \frac{s}{\omega}\right)} \quad \text{max. cyclic kines } \angle, \qquad (23)$$

where

$F = AI =$ the maximum cyclic V.M.F. to standard phase, dynes $\angle$,
$A =$ force constant of the receiver, dynes/absampere,
$I =$ maximum cyclic current strength, absamperes,
$r =$ mechanical resistance of diaphragm, dynes/kine,
$m =$ equivalent mass of diaphragm, gm.,
$s =$ elastic constant of diaphragm, dynes/cm.,
$z =$ mechanical impedance, dynes/kine $\angle$,
$\omega = 2\pi n$, impressed angular velocity, radians/sec.,
$\omega_0 =$ resonant angular velocity, radians/sec.,
$n =$ impressed frequency, cycles/sec.,
$n_0 =$ resonant frequency, cycles/sec.,
$j = \sqrt{-1}$,
$x_m =$ mechanical displacement amplitude of diaphragm, max. cyclic cm. $\angle$,
$x_m =$ vibrational velocity of diaphragm, max. cy. kines $\angle$.

When the vibrating diaphragm supplies motional power to a dependent vibrational system, having its own natural frequency n_{02}, and therefore its own mechanical constants z_2, m_2, r_2 and s_2, the dependent or secondary system will exert a max. cyclic counter vibromotive force (C.V.M.F.) $-f_2$, on the driving force F; so that the resulting equation of motion becomes

[16] Bibliography, 9.

$$\dot{x}_a = \frac{F - f_2}{z} = \dot{x}_m - \dot{x}_2, \qquad \text{kines } \angle, \quad (24)$$

where $\dot{x}_a$ is the max. cyclic velocity of the diaphragm in the presence of absorption. The C.V.M.F. f_2 is proportional to the velocity $\dot{x}_a$, to the mechanical resistance r_2 of the dependent system, and to the relative phase of $\dot{x}_2$ and r_2, as defined by the complex ratio r_2/z_2.

That is,

$$f_2 = \dot{x}_a r_2 \left(\frac{r_2}{z_2}\right) = \dot{x}_a \frac{r_2^2}{z_2}, \quad \text{max cy. dynes } \angle. \quad (25)$$

The secondary C.V.M.F. f_2 will therefore be out of phase with the velocity $\dot{x}_a$ of the diaphragm, except at the frequency n_{02} of secondary resonance, when $z_2 = r_2$; and

$$f_{02} = \dot{x}_a r_2, \qquad \text{max cy. dynes } \angle. \quad (26)$$

Substituting (25) in (24), we obtain

$$\dot{x}_a = \frac{F - \dot{x}_a \dfrac{r_2^2}{z_2}}{z}, \quad \text{max cy. kines } \angle, \quad (27)$$

whence

$$\dot{x}_a = \frac{F}{z + \dfrac{r_2^2}{z_2}} = \frac{F}{z + z_a}, \quad \text{max cy. kines } \angle. \quad (28)$$

The effect, therefore, of the dependent system having a secondary resonant frequency is to add a new *absorption impedance*

$$z_a = r_2^2/z_2$$

to the primary impedance z.

Solving (24) for $\dot{x}_2$ the absorption or secondary velocity we obtain

$$\dot{x}_2 = \left(\frac{F}{z}\right)\frac{z_a}{z + z_a} = \dot{x}_m \left(\frac{z_a}{z + z_a}\right), \quad \text{max cy. kines } \angle. \quad (29)$$

From an examination of (28), it is evident if the primary and secondary frequencies are tuned to coincide, *i. e.*, if $n_{02} = n_0$, then at this frequency, $z_2 = r_2$ and $z = r$, so that

$$\dot{x}_a = \frac{F}{r + r_2}, \qquad \text{max cy. kines } \angle. \quad (30)$$

In this case, the velocity, in the presence of distortion, is in phase with the impressed force at the doubly resonant frequency; but is less than it would be in the absence of the secondary system, in the ratio $r/(r+r_2)$. Moreover, at all other frequencies, the resulting

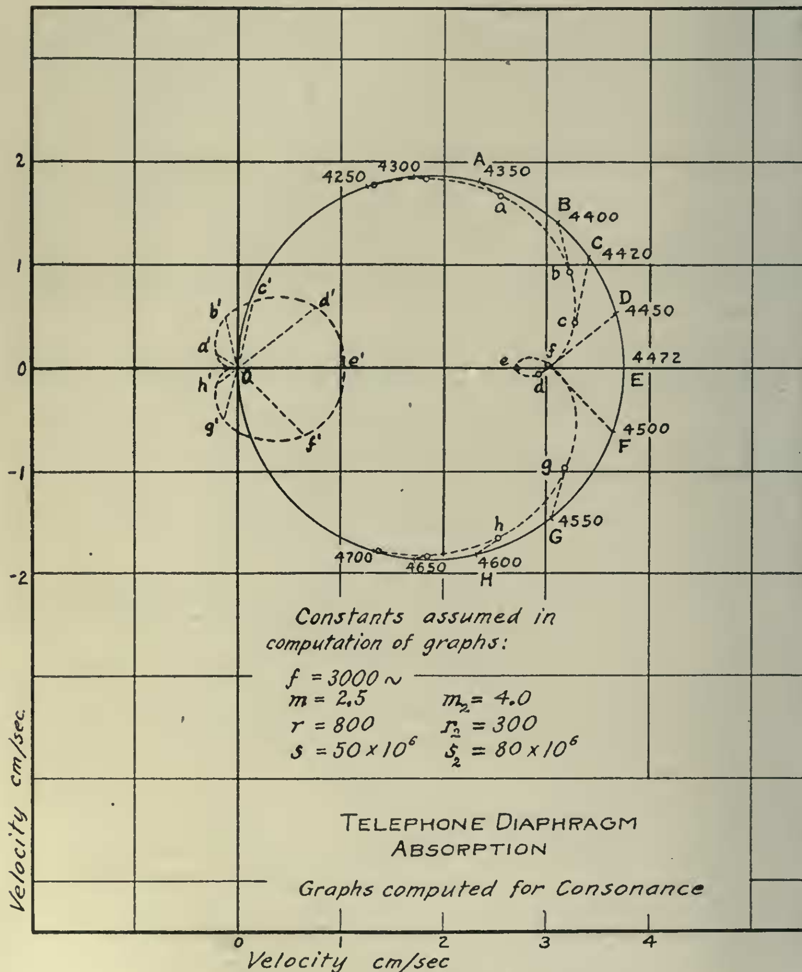

FIG. 20. Computed Distorted Velocity Circle.

velocity $\dot{x}_a$ is less than the normal velocity. The secondary velocity $\dot{x}_2$ is greatest at the doubly-resonant frequency, and falls off rapidly as this frequency is departed from on either side.

Fig. 20 gives the computed graphs for a particular case, where *ABCDH* is the normal-velocity circle $\dot{x}_m$, in heavy line, and *abcdh* of $\dot{x}_a$ is the distorted velocity graph; also $a'b'c'd'h'$ of x_2 is the absorption velocity graph, reckoned negatively. At any impressed angular velocity, such as 4,450 radians per second, the undistorted or primary velocity $\dot{x}_m$ would be OD cm. per sec., leading the impressed V.M.F. by the angle EOD. The observed velocity $\dot{x}_a$, in the presence of distortion, is Od; while the vector difference between the $\dot{x}_m$ and $\dot{x}_a$, or Dd, is equal to $\dot{x}_2 = -Od'$ or Od' reversed.

It will be observed that the graph of x_2, $a'b'c'h'$ is only approximately a circle. It may be regarded, in the light of (29), as the graph of a vector fraction of a motional circle.

It should also be noted from (28) that when the primary and secondary resonant frequencies differ, the resultant velocity $\dot{x}_a$ will not come into phase with the V.M.F. at either resonance frequency, but will trace a dissymmetrical loop. The absorption velocity graph $a'b'c'h'$ will be likewise dissymmetrical.

Fig. 6 shows the observed graph $Oabch$ of motional impedance, and therefore of velocity, with reference to an impressed force in the vector direction OE. The heavy circle $OABCH$ is the inferred undistorted or primary graph, as deduced from the segment AOH. The foliate graph $Oa'b'c'h'$ is the vector difference, or secondary graph of absorption. It will be observed that except for a slight difference in the primary and secondary resonant frequencies, the case presented in this test agrees closely with the geometrical relations indicated in Fig. 20.

Referring to Figs. 7 and 8, it will be observed that the angle AOC is approximately equal to the angle COF. This means that, at secondary resonance, the absorption velocity OF lies nearly as far in angle beyond the vector OC, of that frequency on the undistorted circle, as OC lies from OA the mean diameter. Formula (29) gives a ready explanation for this; because at secondary resonance $z_a = r_2$, so that

$$\dot{x}_2 = \dot{x}_m \left(\frac{r_2}{z + r_2} \right), \qquad \text{kines } \angle. \quad (31)$$

If, as in the cases represented by Figs. 7 and 8, r_2 is small by comparison with z, this becomes approximately

$$\dot{x}_2 = \dot{x}_m \left(\frac{r_2}{z} \right), \qquad \text{kines } \angle. \quad (32)$$

or the vector $\dot{x}_2 = OF$, is displaced from the vector $\dot{x}_m = OC$ by a phase angle equal to the angle of the primary impedance z, which is itself the angle AOC. In other words, the factor r_2/z is a complex quantity whose argument is the negative of that of z. Owing to the presence of r_2 in the denominator of (31), the angular deviation of $\dot{x}_2$ from $\dot{x}_m$ will be always somewhat less than the angle AOC of z; so that the vector CE parallel to FO of secondary resonance, always intersects the diameter OA at a point a little nearer to the origin than the center of the main impedance circle.

The theory also explains why a distortion loop, when the secondary frequency is much below the primary frequency, is very small, and near to the origin on the right; also, as the resonant frequencies are made to approach, the loop enlarges, falling nearer to the main diameter, and finally, as the resonant frequencies pass each other and again diverge, the loop shrinks in size, and passes off towards the origin on the left. In (29), if secondary resonance occurs much above or below primary resonance, the loop due to this resonance will appear remote from the diametrical point A, z_2 again reduces to r_2 and

$$\dot{x}_2 = \frac{F}{z}\left(\frac{r_2}{z + r_2}\right), \qquad \text{kines } \angle, \quad (33)$$

since r_2 is then certainly small by comparison with z, this is approximate to Fr_2/z^2; or varies inversely as the square of the impedance modulus. On the other hand, as the primary and secondary resonances approach, z approaches r, and $\dot{x}_2$ finally attains a maximum possible value at $Fr_2/r(r + r_2)$. If $r_2 = pr$, this becomes

$$\dot{x}_2 = \frac{F}{r}\left(\frac{p}{p + 1}\right) = \dot{x}_m\left(\frac{p}{p + 1}\right), \quad \text{kines } \angle. \quad (34)$$

This shows that in order to have a secondary absorption velocity nearly equal to the primary velocity, it is necessary to have the two resonant frequencies n_0 and n_{02} nearly coincident, and p large by comparison with unity; or the secondary resistance large by comparison with the primary resistance. In such a case, if the two frequencies do not quite coincide, there will be nearly zero velocity and amplitude near to the secondary frequency and a maximum velocity on each side of this, as in Figs. 14 and 15.

Summary.

1. The depression angles $\beta_1{}^0$ and $\beta_2{}^0$ of the diameter of a telephone receiver's motional-impedance circle are not closely connected, and are differently affected by impressed frequency. In some cases $\beta_1{}^0$ was found to be the greater, and in others $\beta_2{}^0$. Increase in frequency increased $\beta_1{}^0$. Neither angle was markedly affected by changes in air-gap. The relations between $\beta_1{}^0$ and $\beta_2{}^0$ may be conveniently studied by means of Lissajous figures.

2. Both the vibration galvanometer, and the oscillograph, have a motional-impedance circle, and a corresponding useful series of motional constants A, m, r and s. Tests were made on well-known types of these instruments, and their theory is outlined in Appendix I.

3. The motional-impedance circle of a telephone receiver may sometimes reveal a distortion, accompanied by an absorption and a suppression of power. The distortion is ordinarily a reëntrant loop. It may also be a general shrinking of velocity, over a considerable range of frequency, accompanying a flattening of the impedance circle.

4. A distortion in the form of a reëntrant loop is attributable to the existence of a secondary or dependent vibratory system, having its own motional constants and resonant frequency. The invading loop may in particular cases be so large as almost to bring the motional impedance to zero near the main diameter. In such a case, there will be two frequencies of markedly large amplitude, one on each side of the frequency of greatest absorption.

5. A distortion in the form of a general flattening of the impedance circle might be accounted for by the existence of secondary vibration in a dependent attached system, not having a definite natural frequency.

6. The dissymmetrical clamping of an amplitude measurer to the cap of a telephone receiver may introduce such deformation of the clamping circle as will give rise to a reëntrant loop or loops. Care should therefore be taken to avoid introducing dissymmetrical stresses when applying such an instrument to a receiver.

7. A dependent motional system, consisting of a short strip spring

fastened to the center of a telephone diaphragm, and tuned nearly into consonance therewith, gave rise to a large reëntrant loop.

8. A provisional but apparently satisfactory theory of loop distortion is given in Appendix II.

9. An experimental form of coupled multiple pendulum is described, which affords a visual manifestation of the essential phenomena of the motional-impedance circle, and of its loop distortions.

10. Means are described for applying a correction for the absorption due to the use of an amplitude measurer, when determining the motional constants A, m, r and s of a telephone receiver.

BIBLIOGRAPHY.

1. M. J. Lissajous. Mémoire sur l'Étude Optique des Mouvements Vibratoires, Annales de Chimie et de Physique (3), p. 147, LI., 1857.
2. Rayleigh. Theory of Sound, Vol. I., p. 147, Macmillan Co., 1894.
3. A. Campbell. On the Measurement of Mutual Inductances by the Aid of a Vibration Galvanometer. *Phil. Mag.*, p. 494, May 14, 1907.
4. E. H. Barton. Text-Book of Sound, p. 146. Macmillan Co., 1908.
5. W. Duddell. Bifilar Vibration Galvanometer. *Phil. Mag.*, pp. 168–179, July, 1909; Electrician, 63, pp. 620–622, July 30, 1909.
6. Frank Wenner. A Theoretical and Experimental Study of the Vibration Galvanometer. Bull. Bur. of Stand., Vol. 6, No. 3, p. 347, Feb., 1910.
7. A. E. Kennelly and G. W. Pierce. The Impedance of Telephone Receivers as Affected by the Motion of their Diaphragms. Proc. Am. Acad. of Arts and Sciences, Vol. XLVIII., No. 6, Sept., 1912; also *Electrical World*, N. Y., Sept. 14, 1912; also British Assoc. Adv. Sc. Report Dundee meeting, 1912.
8. R. L. Jones. Simple Vibratory Systems and their Impedance Analysis. Western Electric Co. Eng. Dept. Report, Sept. 24, 1914.
9. A. E. Kennelly and H. O. Taylor. Explorations over the Vibrating Surfaces of Telephonic Diaphragms under Simple Impressed Tones. Proc. Am. Philos. Soc., Vol. LIV., April 22, 1915.
10. A. E. Kennelly and H. A. Affel. The Mechanics of Telephone-Receiver Diaphragms, as Derived from their Motional-Impedance Circles. Proc. Am. Acad. of Arts and Sciences, Vol. LI., No. 8, Nov., 1915.
11. H. G. Crane and C. L. Dawes. Construction of a Lecture-Room Oscillograph. *Electrical World*, p. 424, Vol. 67, February 19, 1916.

List of Symbols Employed.

A — Torque constant of a vibration galvanometer or oscillograph (dyne-perp.-cm. per absampere). Also force constant of a telephone receiver (dynes per absampere).

$c = n_2/n_1$ — Acoustic interval between quadrantal frequencies (numeric).

Δ — Damping constant, a hyperbolic angular velocity (hyp. radians per sec.).

e_x	Instantaneous emf. opposite and equal to cemf. of motion (abvolts ∠).
$\epsilon = 2.71828$	Base of Naperian logarithms.
f	Instantaneous vibromotive force or torque (dynes) or (dyne-perp.-cm.).
f_1	Force entering into a torque (dynes).
F	Maximum cyclic vibromotive force or torque, (dynes) or (dyne-perp.-cm.).
f_2	Maximum cyclic counter V.M.F. of absorption (dynes ∠).
θ	Angular deflection of vibrator mirror (radians ∠).
θ_m	Maximum angular deflection at resonance (radians).
θ_0	Initial amplitude of angular deflection at moment of release (radians).
θ_s	Steady angular deflection produced by a continuous current (radians).
θ_t	Amplitude of angular deflection at time t after release (radians).
θ	Complex instantaneous angular velocity (radians/sec. ∠).
$\ddot{\theta}$	Complex instantaneous angular acceleration (radians/sec.² ∠).
I	A continuous current strength (absamperes).
I_m	Maximum cyclic current in the vibrator (absamperes).
i	Complex instantaneous current strength (absamperes ∠).
$j = \sqrt{-1}$	
l	Length of radius arm on which a torque acts (cm.).
m	Moment of inertia of vibrating system (gm.-cm.²). Also mass of linear vibration system (gm.).
m_2	Mass of a secondary linear vibration system (gm.).
n	Impressed frequency (cycles per sec.).
n_0	Resonant frequency (cycles per sec.).
n_1	Frequency at earlier quadrantal point in motional circle (cycles per sec.).
n_2	Frequency at later quadrantal point in motional circle (cycles per sec.).
$p = r_2/r_1$	Ratio of secondary to main mechanical resistance (numeric).
$\pi = 3.1416$	
r	Torque of resistance to angular velocity (dyne-perp.-cm./radian per sec.). Also resistance to vibrational motion of a diaphragm (dynes/kine).
r_2	Resistance of secondary or dependent system to motion (dynes/kine).
s	Torque of angular displacement (dyne-perp.-cm./radian). Also elastic constant of linear vibration system (dynes/cm.).
s_2	Elastic constant of secondary linear vibration system (dynes/cm.).
t	Elapsed time (secs.).
τ	Torque (dyne-perp.-cm.).
$\Lambda = \omega_0/2\Delta$	Resonant sharpness, or sharpness of tuning (numeric).

x	Instantaneous displacement of diaphragm (cm.).
x_m	Max. cyclic displacement of diaphragm (cm.).
$\dot{x}$	Complex velocity of diaphragm (cm./sec.).
$\dot{x}_m$	Max. cyclic velocity of diaphragm (cm./sec.).
$\dot{x}_a$	Max. cyclic velocity of diaphragm in presence of absorption (cm./sec.).
$\dot{x}_2$	Max. cyclic complex velocity of secondary system (cm./sec.).
Z	Motional impedance of vibrator (absohms $\angle$).
Z_m	Maximum motional impedance at resonance (absohms).
z	Torque of mechanical impedance to angular velocity (dyne-perp.-cm./rad. per sec. $\angle$). Also force of mechanical impedance to diaphragm velocity (dynes/kine $\angle$).
z_2	Mechanical impedance of secondary system (dynes/kine $\angle$).
$z_a = r_2^2/z_2$	Change of primary mechanical impedance, due to presence of the absorption or secondary system (dynes/kine $\angle$).
$\omega = 2\pi n$	Angular velocity of impressed frequency (radians per sec.).
$\omega_0 = 2\pi n_0$	Angular velocity of resonance (radians per sec.).
$\omega_1 = 2\pi n_1$	Angular velocity of earlier quadrantal point on motional circle (radians per sec.).
$\omega_2 = 2\pi n_2$	Angular velocity of later quadrantal point on motional circle (radians per sec.).
$\omega_d = 2\pi n_d$	Impressed angular velocity producing maximum angular deflection (radians per sec.).
$\omega_f = 2\pi n_f$	Angular velocity of free oscillation (radians per sec.).
$\triangleq$	Nearly equal to.
ab. or abs.	Prefix indicating a C.G.S. magnetic unit.
kine	1 cm./sec.
V.M.F.	Vibromotive force.
$\angle$	Indication of a complex unit.